PHILOSOPHICAL TRANSACTIONS B

royalsocietypublishing.org/journal/rstb

Review

Cite this article: Wan KY, Jékely G. 2021 Origins of eukaryotic excitability. *Phil. Trans. R. Soc. B* **376**: 20190758. https://doi.org/10.1098/rstb.2019.0758

Accepted: 10 November 2020

One contribution of 8 to a theme issue 'Basal cognition: conceptual tools and the view from the single cell'.

Subject Areas:
biophysics, cellular biology, evolution, behaviour

Keywords:
eukaryogenesis, excitability, motility, cilia, membranes, protists

Authors for correspondence:
Kirsty Y. Wan
e-mail: k.y.wan2@exeter.ac.uk
Gáspár Jékely
e-mail: g.jekely@exeter.ac.uk

Electronic supplementary material is available online at https://doi.org/10.6084/m9.figshare.c.5252389.

THE ROYAL SOCIETY PUBLISHING

Origins of eukaryotic excitability

Kirsty Y. Wan and Gáspár Jékely

Living Systems Institute, University of Exeter, Stocker Road, Exeter EX4 4QD, UK

KYW, 0000-0002-0291-328X; GJ, 0000-0001-8496-9836

All living cells interact dynamically with a constantly changing world. Eukaryotes, in particular, evolved radically new ways to sense and react to their environment. These advances enabled new and more complex forms of cellular behaviour in eukaryotes, including directional movement, active feeding, mating, and responses to predation. But what are the key events and innovations during eukaryogenesis that made all of this possible? Here we describe the ancestral repertoire of eukaryotic excitability and discuss five major cellular innovations that enabled its evolutionary origin. The innovations include a vastly expanded repertoire of ion channels, the emergence of cilia and pseudopodia, endomembranes as intracellular capacitors, a flexible plasma membrane and the relocation of chemiosmotic ATP synthesis to mitochondria, which liberated the plasma membrane for more complex electrical signalling involved in sensing and reacting. We conjecture that together with an increase in cell size, these new forms of excitability greatly amplified the degrees of freedom associated with cellular responses, allowing eukaryotes to vastly outperform prokaryotes in terms of both speed and accuracy. This comprehensive new perspective on the evolution of excitability enriches our view of eukaryogenesis and emphasizes behaviour and sensing as major contributors to the success of eukaryotes.

This article is part of the theme issue 'Basal cognition: conceptual tools and the view from the single cell'.

1. Introduction

Cellular excitability is the capacity to generate dynamic responses to stimuli, often over millisecond timescales. An initially weak reaction can be amplified nonlinearly to trigger a strong or impulsive response. Traditionally, the term 'excitability' has been associated with neurons and their electrical properties [1], often manifesting as rapid changes in membrane potential and electrical spiking activity known as action potentials. More generally, however, an excitable dynamical system is capable of supporting not only all-or-nothing responses that are independent of the stimulus amplitude, but also other signal types. These can also propagate spatially, with or without attenuation. An excitable system often undergoes a characteristic excursion through state space, before returning to its original state after a refractory period has elapsed. Here, we invoke this extended definition of excitability to explore cellular phenomena that specifically drive whole-organism behaviour across prokaryotic and eukaryotic cells.

During eukaryogenesis, cells evolved new mechanisms of excitability to sense and react rapidly to their environment. In all cells, excitability is underpinned by the thermodynamics of interfaces. Interfaces are formed by biomembranes that bind regions with different ionic compositions. Excitability emerges as a biophysical consequence of charge separation across biological membranes. This is regulated by the passage of ions between different cellular compartments through ion channels or biochemical signals initiated by metabotropic receptors. These ionic currents then regulate effector systems, including the cilium or contractility apparatus. The ionic homeostasis of the compartments is maintained by active pumping by ATPase pumps [2]. Biosensing is achieved

whenever this homeostasis is disturbed from its equilibrium or steady state, by perturbative influences, which can then propagate rapidly and directionally across the membrane [3].

In general, eukaryotic cells display more complex behaviours than prokaryotes (archaea and bacteria). The differences often are not only quantitative but also qualitative. During eukaryogenesis, radically new forms of sensing and reacting to stimuli have evolved. This enabled deterministic navigation in eukaryotes, particularly direct tracking of gradients or movement along with vectorial cues in three dimensions in open water (3D taxis). Many eukaryotes also actively select particles during feeding, explore substrates, or undergo regulated cell–cell fusion during sex. Phagotrophy is another characteristic that distinguishes eukaryotes from other forms of life.

What are the evolutionary origins of these new forms of behaviour? Are there universal features that we can identify, which clearly set eukaryotes apart from prokaryotes? Here we attempt to trace the evolutionary origins of eukaryotic excitability by invoking a combination of cell biology and physical principles.

This paper is organized into two main sections. We begin with a comprehensive overview of eukaryote-signature behaviours and contrast these to those exhibited by prokaryotes. We proceed to argue that beyond changes in gene complements, several major cellular innovations were likely critical to the emergence of these new forms of behaviour. These all evolved during eukaryogenesis and were likely to have been present in the last eukaryotic common ancestor (LECA). Key structural innovations include changes in the complement of membrane channels, compartmentalization and new types of motility-generating appendages (eukaryotic cilia/flagella and pseudopodia). Furthermore, a general increase in cell size and compartmentalization could have fundamentally changed the biophysical regimes accessible to eukaryotic cells.

In this article, we present a new perspective of how these cellular innovations prompted the 'new physics' that may have unlocked the evolution of new sensory and response strategies that were previously unavailable to prokaryotes. We have organized the paper along clear conceptual lines with the aim of bringing high-level order to a large, sometimes disconnected body of literature. As Henri Poincaré once suggested *'Le savant doit ordonner …'* [4].

2. Forms of excitability in eukaryotes

In this section, we give an overview of the forms of excitability, sensing and response that are characteristic of eukaryotes, and contrast these strategies with those encountered in prokaryotes. We first focus on single-cell strategies for tactic navigation. Self-locomotion, or motility, is an important feat that not only increases the efficacy of environmental exploration, but also enables cells to move toward more favourable environments, and away from harm. Motility control in the presence of spatio-temporal gradients is an ideal testbed for evaluating a cell's sensory performance. Apparently very different microscopic sensorimotor rules can nonetheless lead to similar macroscopic or end outcomes, namely, some form of net migration towards or away from a stimulus.

Among motile organisms, strategies for navigation are often diverse and highly organism-specific. There are three major strategies for cells to track gradients of external cues (e.g. chemicals, light, temperature), which we shall refer to as stochastic navigation, spatial sensing and helical klinotaxis. This is inspired by the classification of Dusenbery [5], and also similar to the convention adopted by Alvarez *et al.* [6] in the context of chemotaxis. We shall seek to understand how the propensity for prokaryotes and eukaryotes to adopt different strategies may have arisen from adaptations to different physical regimes.

In addition, there are passive forms of orientation, which we will not discuss in detail here. These include magnetotaxis in some proteobacteria and a euglenid alga [7–9]. There are further idiosyncratic forms of environmental tracking that do not fall into any of the above navigation categories, such as active regulation of buoyancy in non-motile diatoms in order to move up and down in the water column [10,11].

With the advent of enhanced sensory and navigational capabilities, eukaryotes became capable of more sophisticated behavioural sequences (summarized in figure 1 and table 1). These include nonlinear responses to mechanical stimulation and complex membrane dynamics, including cell engulfment and cell–cell fusion. Orderly sequences of excitable actions manifest themselves in the everyday processes in the life of a eukaryotic cell, for example, chemosensing or tracking of other cells by chemotaxis, followed by engulfment (phagocytosis) or cell fusion (sex).

(a) Stochastic or non-oriented navigation

The response of an organism or cell to stimuli is not always directional. Instead *stochastic navigation* strategies—also termed *kineses*—exist (figure 1*a*). This form of navigation is most widespread among prokaryotes but also occurs in some eukaryotes. Stochastic navigation is a form of temporal sensing, during which changes in the concentration, e.g. of a chemical, are detected as the cell moves along a gradient. The most common strategy among prokaryotes consists of straight runs followed by brief turns [12] or tumbles to reorient the trajectory [13]. During positive chemotaxis, a sufficient rate of increase in the chemoattractant concentration will suppress tumbles, biasing the movement up the gradient [14]. Run-and-tumble chemotaxis does not involve directed turns and can therefore be referred to as statistical or indirect chemotaxis [5], or *chemokinesis*. Variations include run-and-reverse, run–reverse-and-flick [15] or run-and-stop [16]. It has been reported that some polarly flagellated bacteria exploit a buckling instability to steer, producing a peaked distribution around preferred turning angles [17]. These kinetic strategies depend on two-component signalling and generally apply to bacterial and archaeal chemotaxis and phototaxis [18,19]. Cells achieve biased migration according to generalized velocity-jump random walk processes [20].

Stochastic trial-and-error navigation by temporal sensing also exists among eukaryotes but is not as well-characterized. Recently, it was shown that aerotaxis (tracking of oxygen gradients) in choanoflagellates relies upon such a stochastic navigation strategy [21]. A similar mechanism operates during phototaxis in the pico-eukaryote *Micromonas* [22]. Many ciliates are capable of multiple gradient sensing strategies which may include a stochastic component, depending on the nature of the stimulus or irritant. Bacterial chemoattractants can also stimulate chemokinesis in *Tetrahymena*, leading to an increase in swimming speed [23]. The capacity for chemoattractants (e.g. glutamate, folate) and chemorepellents

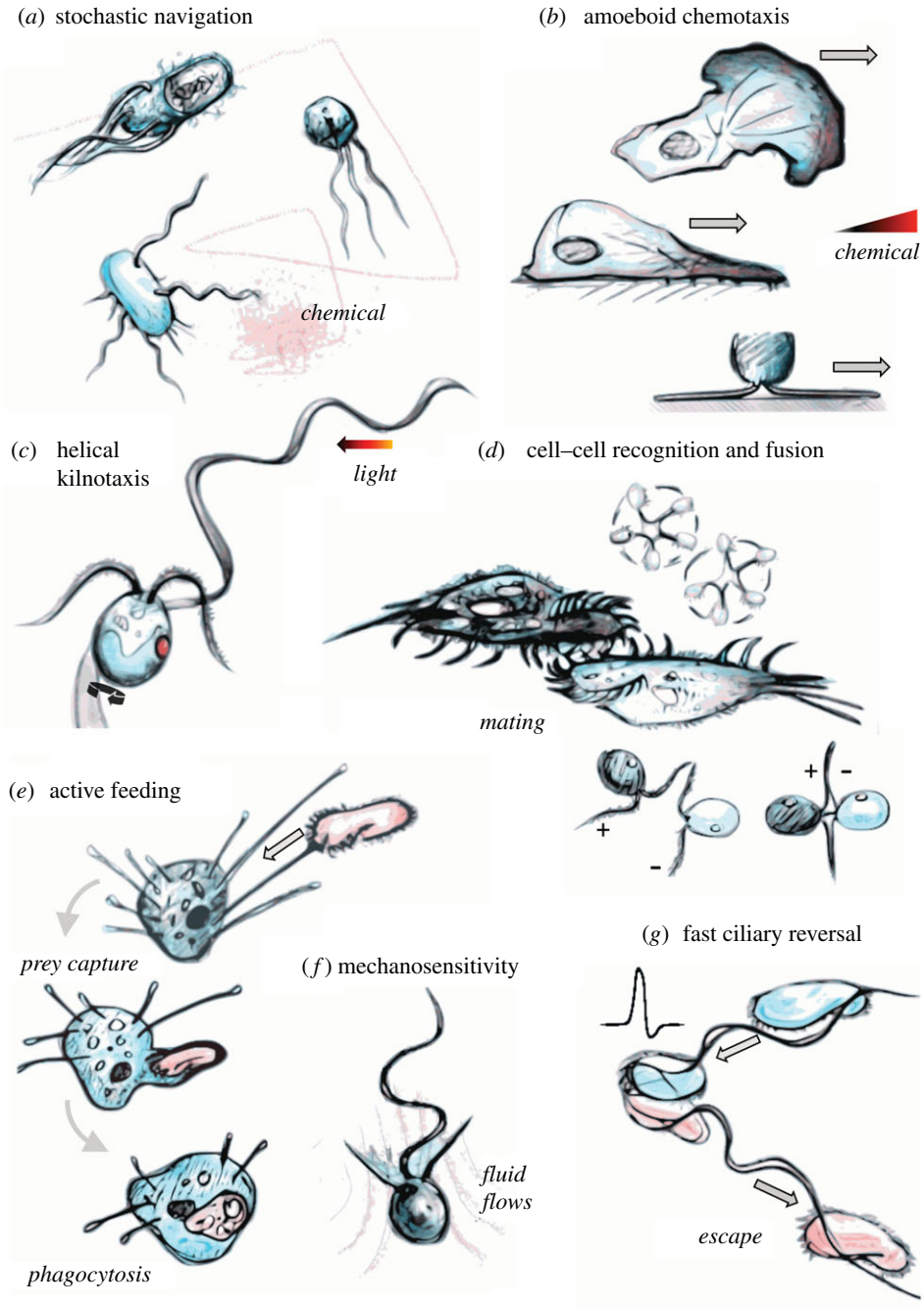

Figure 1. The many forms of cellular excitability. (*a*) Stochastic or non-oriented navigation strategies (e.g. prokaryotic chemotaxis), (*b*) sensing by spatial comparison (e.g. amoeboid chemotaxis), (*c*) sensing by helical klinotaxis (e.g. flagellate phototaxis), (*d*) cell–cell recognition as a prelude to fusion (e.g. ciliate conjugation and gametic fusion in *Chlamydomonas*), (*e*) active feeding by selective engulfment of prey organisms, (*f*) mechanosensitivity and flow interactions, and (*g*) ultrafast escape responses and reversal of ciliary beating by action potentials. (Online version in colour.)

(toxins) to induce positive and negative kinetic effects in ciliates including *Tetrahymena* and *Paramecium* is well-established [24,25]. Different chemical signals induce a combination of more subtle movement responses, including klinokinesis (random reorientations) and orthokinesis (changes in speed). When exposed to extracellular GTP, some ciliates exhibit repetitive back-and-forth motion, a more complex form of excitability mediated by membrane potential [26].

(b) Deterministic steering by spatial comparison

In contrast with stochastic kineses, organisms can also tune their orientation with respect to a cue. Taxes are further subdivided [27] into *tropotaxis*, when gradients are measured directly at two different locations at the same time (spatial sensing), usually requiring at least two spatially separated receptors, and *klinotaxis*, when gradients are measured sequentially at two different times (temporal sensing) at the same receptor, while the organism is in motion (see §2c).

Sensing by spatial comparison (figure 1*b*) is a form of navigation that is a eukaryotic characteristic, with a few exceptional prokaryotic cases. Spatial chemosensing or light sensing relies on the differential excitation of one part of a cell coupled to directional movement along a gradient or vector. Among eukaryotes, spatial chemosensing is widespread across many supergroups and possibly traces back to the LECA. Most amoeboid eukaryotes are thought to perform chemotaxis through spatial sensing [28].

Amoeboid cells migrate by directional chemotaxis towards bacteria or other food sources. The mechanism is spatial sensing coupled to the directional extension of pseudopodia [29]. Such amoeboid chemotaxis has been demonstrated in members of many eukaryotic clades. Amoeboid cells of the excavate amoeboflagellate *Naegleria fowleri* (Discoba, Heterolobosea) show chemotaxis towards bacteria [30]. Similar directed chemotactic migration is present in *Acanthamoeba* [31], *Entamoeba* [32], *Hartmannella* [33], *Dictyostelium* and amoeboid cells in animals [29]. Directional chemotaxis also functions in syncytial forms like the plasmodia of the slime mould *Physarum* [34].

Chemotaxis in *Dictyostelium* is perhaps the best studied from a biophysical perspective [35]. In the absence of gradients, pseudopods extend randomly, but extensions become localized when gradients are detected. Cells can sense gradients of only 2% front-to-back and can migrate towards travelling waves of chemoattractant [36]. In very shallow gradients, cells extend pseudopodia stochastically and retain the ones oriented towards a source of chemoattractant [37]. *Dictyostelium* can also reconfigure its motility machinery to migrate against shear flows [38,39]. This active response relies on spatial sensing of differential hydrodynamic forces; just as during chemotaxis, directional pseudopodial motility occurs by an actin-polymerization-dependent mechanism.

There are other—likely more derived—forms of tropotaxes among eukaryotes. The euglenoid *Peranema* glides on surfaces and can efficiently move towards sources of food [40]. A long anterior flagellum and a short ventral flagellum are attached to an elongated cell body—which is itself capable of amoeboid-like movement in the absence of the flagella. Gliding by cilia is present in many species and relies on a surface mechanism mediated by interactions between transmembrane proteins and the substrate [41]. Red algae glide on surfaces and can move towards light by directional steering [42,43]. Since red algae generally lack cilia and helical swimming, their phototactic movement may rely on spatial sensing (shading or focusing by lipid droplets) and directional growth of cellular protrusions [44]. Filamentous eukaryotes with cell walls show directed orientation or growth along chemical gradients, including fungal hyphae [45], the pollen tube of plants [46] and plant roots undergoing hygrotropism [47].

Prokaryotes display spatial sensing only very sporadically or only as collectives. Multicellular communities of some bacteria display collective behaviour reminiscent of deterministic tracking by spatial comparison. Swarming *Pseudomonas aeruginosa* can track chemical trails by collective movement, even if the individual bacteria only move randomly [48]. Swarm colonies of the bacterium *Rhodospirillum centenum* show directional phototaxis through an unknown direction-sensing mechanism, possibly exhibiting colony-level shading [49,50]. *Myxococcus xanthus* swarming on agar plates turn towards plastic and glass beads by sensing deformations in surface texture (elasticotaxis) [51–53].

At the single-cell level, prokaryotes are too small for spatial sensing to be effective (§2f), with few exceptions. Some relatively large (2 × 6 µm) bipolar flagellated vibrioid bacteria (identified as *Thioturbo danicus* [54]) can track steep oxygen gradients and perform directional turns, likely by spatial sensing [55]. The cells are able to detect oxygen gradients across a distance of several micrometres along their long axis. Turning may rely on the faster rotation of the flagellar bundle at the cell pole exposed to higher oxygen levels. Another unusual form of spatial sensing is found in the cyanobacterium *Synechocystis*, which is able to follow directional light cues. These cells act as spherical microlenses to focus incoming light to the opposite side of the plasma membrane. This localized stimulus induces motility in the direction of light [56]. A further interesting example is presented by *Pseudoalteromonas haloplanktis* and *Shewanella putrefaciens*. These bacteria appear to steer towards and track individual free-swimming algae [57]. However, tracking may not be due to deterministic steering behaviour and can be explained by fluid dynamical effects due to the algal cell's vorticity field [58].

(c) Deterministic steering by temporal comparison

Klinotaxis relies on temporal comparisons and chiral self-motion (figure 1*c*). This is arguably the most sophisticated of cellular navigation strategies and occurs almost exclusively in eukaryotes. Helical self-propulsion at low Reynolds numbers arises naturally when cell-shape asymmetries are combined with periodic stroke patterns (e.g. of cilia and flagella) [59,60]. Direct taxes employing temporal sensing require the helical trajectories to have sufficiently large amplitude, as found in most freely swimming eukaryotes. During helical turns in a stimulus field, the cell tracks periodic changes in the stimulus, particularly in the direction perpendicular to the helix axis. By bending the helical trajectory in the stimulus direction, the cells can actively steer and migrate deterministically. Thus, helical klinotaxis is fundamentally different from stochastic navigation [5,6], and generally both more efficient and more robust to noise than other navigation types.

Diverse eukaryotes from distinct phyla use helical klinotaxis to track chemical gradients (such as diffusing from a food source) [61]. Helical klinotaxis has been described in various ciliates, the gametes of brown and green algae [62,63], the non-photosynthetic green alga *Polytomella magna* [64], animal sperm [65], fungal zoospores [66], the heterotrophic flagellates *Cafeteria* [61] and *Euglena* [67] and the dinoflagellate *Peridiniopsis berolinensis* [68]. The gametes of many organisms are also guided by helical chemotaxis for external fertilization [69].

A special form of chemotaxis is a prelude to gametic fusion. The helical klinotaxis of flagellated male gametes towards female gametes is common. Since cilia [70], meiosis [71] and thus gametogenesis trace back to LECA, it is possible that the gametes of LECA found each other by helical klinotaxis before sex. In order for gametes to interact, they are often attracted to each other by pheromones—likely some readily diffusible substance. This attraction has been extensively studied in species of brown algae. When the female gametes of brown algae settle on a surface, they secrete sexual pheromones (olefinic C_{11}-hydrocarbons) [72,73], which attract the much more motile, biflagellated male gametes. The male gametes can either swim freely in three-dimensional helical trajectories, or swim close to the surface, moving in two-dimensional circular paths (referred to as thigmotaxis). The chemoattractant pheromones influence the beat pattern of the flagella, increasing the curvature of the helical swimming path [74]. Helical klinotaxis is also adopted by monoflagellated gametes, including fungal zoospores and animal sperm. The male gametes of the aquatic fungus *Allomyces* swim in a helical path interrupted by 'jerks'. The female gametes show little motility and secrete a pheromone (sirenin) that influences the swimming trajectories of male gametes, in order to guide their directional swimming [66].

In other examples of gametic attraction, it is not yet clear whether the mechanism involves helical klinotaxis or stochastic chemokinesis. When both partners are motile, chemoattraction need not be unidirectional. In the ciliate *Blepharisma japonicum* [75] single cells swim more slowly with increasingly circular trajectories around higher concentrations of gamone. Each partner can secrete a different pheromone, which has the potential to attract cells of the opposite mating type. In *Spirostomum* and *Euplotes*, characteristic pre-conjugation rituals ('courtship' or even mating dances) have been described [76,77].

While chemical or thermal gradients are diffuse, other classes of physical stimuli (such as light, gravity, flows) are inherently directional. Phototaxis is a particularly striking example of helical klinotaxis [78]. It likely evolved at least seven times independently during eukaryotic evolution and may not have been a property of the LECA. However, as a biophysical strategy, it is uniquely eukaryotic and was enabled by eukaryotic cellular organization, excitability and movement pattern.

For example, the biflagellate alga *Chlamydomonas* has a single eyespot which leads to an eightfold separation in perceived intensity from one side compared with the other [79]. A non-planar beat pattern leads to a helical trajectory which allows the organism to continuously scan three-dimensional space and modulate the helix axis towards or away from the light. A similar strategy of helical phototaxis can be found in other protists, including *Euglena*, brown algal swarmers and chytrid zoospores (reviewed in [78]).

In the colonial alga *Volvox carteri*, movement of thousands of flagella—which operate as individuals—achieves colony-level phototaxis by virtue of their common stimulus-response function and positional distribution on a spherical body [80]. In *Euglena*, the interplay between eyespot sensor placement and an intensity-dependent reorientation strategy leads to more complex responses to patterned light [81,82].

The most extreme examples of light sensing in a single eukaryotic cell are found in certain predatory dinoflagellates that have large and highly unusual 'camera eyes', called ocelloids—built from endosymbiotically acquired components. This unique organelle has superior light-gathering optics and can refract light to a retina-like structure [83,84]. In the warnowiid dinoflagellate *Erythropsidinium*, the design and sophistication of its eye suggests that it can do more than sense light gradients (as in most other protist photoreceptors) [85]. Ocelloid eyes are even capable of an active rolling or pivoting motion [86]. It is suggested that they can detect circularly polarized light—a tell-tale sign of prey dinoflagellates (polarotaxis). This extraordinary sensory capacity coincides with an arsenal of cellular weapons (e.g. harpoons, nematocysts) which this organism uses to impale its prey. The klinotaxis mechanism in this case must be highly refined, though the connection between signal and action on the flagellar beat pattern is unclear.

In contrast with its widespread use in eukaryotes, klinotaxis is largely absent from prokaryotes. Even though many prokaryotes move in a helical fashion [87,88], this alone is not generally sufficient for klinotaxis, as the radius of the helix must be large enough to allow sampling of gradients (see §2e). Perhaps the only example of true taxis in bacteria occurs in the large sulfide-oxidizing proteobacterium *Thiovulum majus*. *Thiovulum* cells are unusually large for a bacterium (5–25 µm) [89] and can swim at a speed of up to 615 µm s^{-1}, one of the fastest swimming speeds ever recorded for a bacterium [90]. *Thiovulum* cells swim with multiple flagella in a left-handed helix and can directly track a gradient of oxygen by bending the helical trajectory as a function of changes in concentration [91]. Large groups of *Thiovulum* cells also form large-scale fronts owing to their chemotactic behaviour [92].

(d) Cell–cell recognition as a prelude to fusion

Sexual cycles consisting of meiosis and complete cell–cell fusion are unique to eukaryotes. From the perspective of excitability, the key properties of sex are the specific attraction and recognition by gametes, their complete fusion and the prevention of multiple rounds of fertilization. Eukaryotes undergo complete cell–cell fusion during sex and orchestrate this process with remarkable precision.

Mating starts with chemoattraction, often mediated by pheromones and helical klinotaxis (see §2c above). Adhesion and fusion are regulated by genetically determined mating types [93]. In the ciliate *Euplotes patella*, which expresses six mating types and at least three different pheromones (gamones), this attraction is thought to be combinatorial [94]. Gamete recognition can be accompanied by dramatic changes in behaviour. In *Paramecium*, there is a marked reduction in swimming speed following recognition [95]. In the biflagellate alga *Chlamydomonas*, cells of opposite mating type collide randomly, before fusing to form quadriflagellate zygotes. Adhesion occurs via different mating-type-specific glycoproteins expressed on the flagella (agglutinins) [96].

Cilia and flagella often participate in cell–cell fusion as mating organelles (figure 1*d*). In *Paramecium aurelia*, conjugation begins with the adhesion of specific cilia, and cells become adhered at the anterior-ventral side [97]. Membrane fusion then occurs, at surfaces where cilia degenerate, and pores form to provide cytoplasmic bridges between the partners. In *Chlamydomonas*, isogamous gametes of opposite mating types adhere head-to-head along the length of their flagella, with the eyespots on the same side of the cell [98]. The plus mating type then extends a tubular, actin-based mating structure which fuses with a smaller structure in the minus mating type. The temporary quadriflagellate dikaryons are also phototactic [99]. In *Chlamydomonas*, flagellar adhesion is also light-sensitive, in fact light switchable [100], which may explain the necessity of light for gametogenesis in this organism [101]. In oogamous brown algae, the male gametes attach to the female gamete with their anterior flagellum [102]. After one gamete fuses, the others are excluded. This is ensured by the formation of a fertilization barrier by the fusion of Golgi-derived vesicles underlying the plasma membrane [102]. It is unclear if initial chemotaxis and subsequent agglutinative contact are separate processes.

Among prokaryotes, cell–cell fusion is rare, and mostly only incomplete and reversible. In some haloarchaea, the exchange of genetic material can occur through incomplete cell–cell fusion, during which cells are connected by cytoplasmic bridges [103]. The selectivity of the mating process is regulated by surface glycosylation in *Haloferax volcanii* [104]. Among bacteria, transient outer membrane fusion has been observed in the myxobacterium *Myxococcus xanthus* [105]. Among cells of the spirochaete *Borrelia*, frequent outer membrane fusion and occasional inner membrane fusion were observed [106]. A recent study reported complete interspecies cell–cell fusion with large-scale exchange of

cellular components between the bacteria *Clostridium ljungdahlii* and *Clostridium acetobutylicum* [107].

(e) Active feeding by selective engulfment

Another key trait of eukaryotes is predation by whole-cell engulfment, which is often proposed as one of the main innovations driving eukaryogenesis [108,109], an idea not without its critics [110]. Particles or even whole cells primed for engulfment may need to be first brought to a food vacuole by interception, by track-and-capture or by active filtration of self-generated currents [111].

Chemoattractants function to draw predators to prey, followed by specific and ordered activity sequences prior to prey engulfment, which may include cell attachment and the formation of specialized cellular protrusions. In the slime mould *Dictyostelium*, a G-protein-coupled receptor (GPCR), folic acid receptor 1, recognizes both diffusible chemoattractants and surface molecules of bacterial prey [112,113]. The dinoflagellate *Oxyrrhis marina* uses a mannose-binding lectin as a feeding receptor for recognizing prey [114].

In many cases, phagotrophic predators have highly specialized feeding strategies. The heliozoan *Actinophrys sol* can intercept and consume ciliate prey as large as itself by adhering to the ciliate with pseudopod extensions called axopodia, which then wrap around to completely enclose the prey [115]. Many protists possess specialized structures to facilitate prey immobilization and capture [116,117]. Phagotrophic euglenids actively shovel and manipulate prey organisms toward feeding grooves. The freshwater eukaryovorous euglenid *Heteronema* has been described to ensnare *Chlamydomonas* cells whole, by coordinating the action of multiple hook-bearing and mucus-covered flagella into the flagellar pocket [118]. The euglenid *Peranema* uses feeding rods to first pierce prey cells [119], before sucking out their contents directly into a feeding vacuole (*myzocytosis*). Photoautotrophic or osmotrophic species have much more reduced feeding apparatuses. Some dinoflagellates make use of a pseudopodial pallium to envelop and engulf large and awkwardly shaped prey (e.g. diatoms) [120].

Most ciliates, despite having an ordered and largely rigid structure (pellicle), restrict phagocytosis to a single expandable feeding cavity. This structure, known as the cytostome, is often decorated with a ring of specialized cilia. After first paralysing its prey with toxicysts, *Didinium* can engulf and pass a *Paramecium* cell as large as itself through its cytostome [121,122]. This process is associated with calcium-dependent electrical activity [123]. Hypostome ciliates make use of a cylindrical cytopharyngeal basket, which constricts to pass its filamentous prey (e.g. cyanobacteria) into a coil deep within the cytoplasm, at rates of up to 15 $\mu m\ s^{-1}$ [124]. This is accompanied by rapid incorporation into the developing food vacuole of new membrane recycled from vesicular fusion. Generally, the feeding cavity must enlarge and acidify before the prey can be digested [125].

In filter feeders, ensembles of cilia and flagella coordinate to pump fluid at relatively high speeds (up to 1 $mm\ s^{-1}$), often sweeping particles directionally into a feeding apparatus [126]. In collared choanoflagellates and the sessile ciliate *Vorticella*, food particles are sorted by size. In other species, mechanical filtration may be supplemented by adhesive surfaces for added particle selectivity.

Predatory behaviour also exists in prokaryotes [127], but owing to their inability to engulf, proceeds in a very different way. Predatory bacteria generally inflict chemical lysis upon prey cells, or attack collectively. Single-cell strategies are rare. *Bdellovibrio* hunts bacteria [128] but the tracking mechanism does not appear to be chemosensory but rather dependent on hydrodynamic entrapment [129]. A newly described planctomycete [130] can engulf other bacteria and pico-eukaryotes, via a mechanism that resembles but is not thought to be homologous to eukaryotic phagocytosis. However, this is a singular system which is not distributed among prokaryotes.

(f) Mechanosensitivity and flow interactions

Eukaryotes are particularly susceptible to mechanical stimuli and changes in membrane geometry. Many eukaryotes exhibit mechanosensitivity. This allows them to respond actively to hydromechanical signals transmitted remotely through the fluid, without need for direct contact with a potential predator or prey [131–133]. Marine ciliates can perform powerful jumps in response to predator-induced feeding currents at shear rates (magnitude of flow velocity gradients) of 1–10 s^{-1} [134,135].

More graded responses to mechanical cues are controlled by specialized ion channels and transmitted directly through the membrane [136]. These may be localized to cilia and flagella, which display an active load response [137,138]. Hair-like extensions of cilia (mastigonemes) are also implicated in mechanosensing in *Chlamydomonas* [139]. A combination of rheosensing and chemosensing guides sperm motility through the mammalian oviduct. *Dictyostelium* reorients actively to shear flows, i.e. gradients in flow velocity [38].

The mechanosense is also manifest in gravitaxis, as well as gyrotaxis—the interaction between motility, gravity and hydrodynamic torques in many marine protists. In the ciliate *Loxodes*, active control of membrane potential and statocyst-like organelles is thought to determine the sign of gravitaxis [140,141]. Some protists have also adapted to life in the ocean by exploiting sharp vertical gradients and undergoing ballistic diel migration [142]. The gravity-sensing mechanism remains unclear, but is likely to involve a passive shape-dependent mechanical component [143], in addition to active regulatory mechanisms.

Planktonic microorganisms show a great deal of resilience against turbulent ecosystems [144]. For this they must be able to integrate and respond to multisensory information: such as light, chemicals, flows and gravity. Such single-cell responses can lead to large-scale population structures such as algal blooms, even formation of photo-gyro-gravitactic bioconvection patterns and instabilities [145,146]. In general, behavioural transitions are mediated by stimuli-dependent ionic currents and an excitable membrane, coupled to some form of self-locomotion. Cross-responses are even possible (where one type of stimulus elicits a change in the cell's response to another stimulus type). The male gametes of brown algae switch the sign of phototaxis from positive to negative when exposed to chemoattractants [147]. Self-movement in a fluid will alter local gradients, providing an opportunity for reafferent feedback.

Prokaryotes may be too small to respond actively to shear flows. Bacterial rheotaxis (reorientation to shear flow) has been shown to be a passive phenomenon [148]. However bacteria are capable of osmoregulation and do possess ion channels which sense membrane tension [149], and

mechanosensation in *Escherichia coli* has been demonstrated to rely on voltage-induced calcium flux [150]. The torque produced by the flagellar motor (therefore rotation speed) is also load-dependent [151,152]. Other appendages (e.g. pili) for surface movement are candidate mechanosensors and may reflect adaptation to substrate adherence for community living and biofilm formation [153].

(g) Escape responses and action potentials

Stimuli that have the potential to harm or kill demand more immediate detection. This is fundamentally distinct from navigation or exploration, in terms of the timescales available for response. Most motile species harbour a form of phobic or emergency response distinct from their steady state locomotion. Escape reactions are not strictly oriented—but commonly involve backward movement, sometimes with a negatively geotactic component [154]. Additional chemical self-defence strategies may be deployed, for example extrusion of trichocysts by *Paramecium* [155] or ejection of extrusomes in other ciliates [156].

In flagellate algae, abrupt changes in light intensity or intense photic stimuli induce rapid flagellar reversal and transient backward swimming [85,157]. In green algae, this action may be mediated by the contractile root fibre which alters the angle between basal bodies [158]. Cells can also react at speed to unexpected mechanical stimuli. All-or-none contractions in the stalked ciliate *Vorticella* can occur at rates of 8 cm s^{-1} [159]. In some species of heliozoa, axopods can completely retract within 20 ms in order to draw in trapped prey for phagocytosis [159,160].

These fast reactions are usually induced by action potentials—unidirectional electrical pulses involving fast, regenerative changes in membrane potential. While all cells display some electrical activity, phylogenetic evidence suggests that the capacity to propagate action potentials may have been an ancestral eukaryotic trait supported by the LECA. These may have emerged in response to accidental membrane damage and sudden calcium influx [161]. Bioelectrical signalling in the form of action potentials occurs orders of magnitude faster than any other signalling modalities, e.g. chemical diffusion, protein phosphorylation etc.

In order to initiate fast escape responses, these may have been coupled directly to the motility apparatus—particularly to flexible, membrane-continuous structures such as cilia and pseudopodia. Loss of voltage-gated sodium/calcium channels is further correlated with loss of cilia in many taxa. In protists, all-or-none action potentials occur almost exclusively in association with ciliary membranes [162–164], with the exception of some non-ciliated diatoms [165,166]. Graded potentials occur in amoebae, also for movement control [167].

In *Chlamydomonas*, action-potential-like flagellar currents induce photophobic responses and flagella reversal (via the voltage-gated calcium channel Cav2), while photoreceptor currents elicit much milder responses [168]. Here, a mechanosensory channel of the transient receptor potential (TRP) family (TRP11) is localized to the ciliary base, while Cav2 is localized only to the distal regions of cilia [169,170]. In *Paramecium*, hyperpolarizations increase ciliary beat frequency, while depolarizations have the opposite effect and eventually lead to a ciliary reversal. Depolarizations above a certain threshold result in action potentials, owing to opening of Cav channels located exclusively in the ciliary membrane [171,172]. Potassium channels—also residing in the membrane—help restore the resting membrane potential.

Eukaryotes manipulate their membrane potential to achieve transitions between different behaviours. Complex bioelectric sequences have been recorded in association with integrated feeding and predation behaviours in *Favella* [173]. Repetitive behaviours arise from rhythmic spiking. In ciliates, rhythmic depolarizations control fast and slow walking by tentacle-like compound cilia called cirri [174], enabling escape from dead ends [175] and courtship rituals in conjugating gametes [77,94]. In *Stentor*, action potentials produce whole-body contractions [176]. Finally, excitable systems operating close to bifurcations may admit limit cycles, which manifest as repetitive or rhythmic electrical spiking and repetitive behaviours. Ultimately, this may lead to habituation [177,178].

In prokaryotes, action-potential-like phenomena have been observed in biofilms [179] and also single cells. The archaeon *Halobacterium salinarium* shows a photophobic response characterized by a 180° reversal of its swimming direction induced by a reversal in the direction of flagellar rotation. At least some aspects of this response are likely mediated by changes in membrane potential by bacteriorhodopsin, a light-driven proton pump [180]. Action potential-like phenomena in prokaryotes are dissimilar from classical eukaryotic action potentials. The former are less reproducible, slower and exhibit a broader distribution in pulse amplitude and duration [150] (table 1).

3. Cellular and biophysical innovations underpinning eukaryotic excitability

In this section, we give an overview of the cellular innovations that contributed to the emergence of new forms of excitability during eukaryogenesis. These are (i) an extended repertoire of membrane receptors, channels and pumps, (ii) motility by cilia and pseudopodia, (iii) endomembranes and mitochondria as ionic compartments and intracellular capacitors, (iv) a flexible and reconfigurable membrane, (v) a larger size, (vi) new strategies for sensing. We identified these features as of major significance for the origin of eukaryotic excitability, but the list may not be exhaustive. We discuss how these factors contributed to the novel forms of excitability highlighted in the preceding sections and how they underpin new regimes of cellular biophysics that are only accessible by eukaryotic cells.

We shall embed our discussions within the most generally accepted framework for eukaryogenesis. This starts with an archaeal host related to the Asgard archaeal lineage [181]. This host acquired the mitochondrial symbiont—related to alphaproteobacteria—by internalization. There are several versions of this model, and from our perspective, some of the most intensely debated details are less relevant (e.g. how early or late and through which intermediate stages did mitochondria evolve) [182]. We focus here only on the key eukaryotic novelties of membrane topology, motility, ionic currents and other ingredients necessary for excitability, and how these may be contrasted with prokaryotic cell biology. Of note, there are also alternative—and in our view less plausible—cell evolution scenarios for eukaryogenesis, e.g. involving three symbiotic partners [183], which we will not consider here.

Table 1. Forms of cellular excitability in eukaryotes are contrasted with those in prokaryotes. See main text for references.

forms of cellular excitability	prokaryotic examples	eukaryotic examples	made possible by
stochastic navigation	bacterial and archaeal chemotaxis, archaeal phototaxis	choanoflagellate aerotaxis, chemokinesis in some ciliates and flagellates, *Micromonas* phototaxis	any moving appendage or motility mechanism
spatial sensing	*Synechocystis*, *Thioturbo danicus*	amoebae, ciliates	spatially located sensor, large cell size
temporal taxes	*Thiovulum*	helical photo- and chemotaxis across eukaryotes	helical/chiral self-motion, fine motor control over cilia or flagella, temporal sensing, memory
cell fusion	some haloarchaea (incomplete), *Borrelia* (mostly OM, incomplete), *Clostridium* spp. (complete)	all gametic fusion events	cell–cell recognition, adhesion, in most eukaryotes mediated by cilia/flagella
active feeding by engulfment	some planctomycetes	many eukaryotic phagotrophs	deformable membrane, cell recognition, sometimes by specialized appendages, internal digestion
mechanosensitivity and flow interactions	osmosensation	many eukaryotes	mechanosensory channels (e.g. transient receptor potential), membrane fluidity
escape responses and action potentials	cable bacteria, some biofilms	many eukaryotes	voltage and calcium channels (e.g. Cav, Nav), often localized to cilia/flagella

(a) An expanded repertoire of ion channels, pumps and membrane receptors

In eukaryotes, there is a vastly expanded repertoire of membrane channels, pumps and receptors, distributed across a highly compartmentalized cell. Comparative genomics indicates much of this diversity evolved during eukaryogenesis in stem eukaryotes and was present in the LECA (e.g. [184]).

The various fast and slow ionic currents generated by receptors and ion-selective channels underlie the responses of eukaryotic cells to diverse sensory stimuli and injury. The regulation of motility, contractility, mechanosensation, tactic and temperature responses all rely on membrane excitability. The complexification and diversification of ion channels and receptor pathways was one of the major innovations that underpinned the evolution of the new forms of excitability in eukaryotes. In parasites, this diversity can be dramatically reduced. In parasitic trypanosomes, voltage-gated channels are represented by one type, a reduction from ten types in their free-living relative *Bodo saltans* [185].

The regulation of calcium signalling illustrates the exuberance of systems eukaryotes evolved to control the flux of a single ion. Its influx and extrusion are regulated by various types of Ca^{2+} channels and pumps, including store-operated Ca^{2+} channels [186], Ca^{2+} ATPases, and voltage-gated, ligand-gated or mechanosensitive Ca^{2+} channels, including TRP channels.

The levels of free calcium are low in the cytoplasm and high in the endoplasmic reticulum (ER). Intracellular Ca^{2+} is kept low by the action of the plasma membrane calcium-transporting ATPase (PMCA), which counters the influx of Ca^{2+} at the plasma membrane. The influx of Ca^{2+} into the ER in turn is controlled by the sarcoplasmic/endoplasmic reticulum calcium ATPase Ca^{2+} pumps (SERCA). The ER and plasma membrane calcium systems are interlinked. The activation of plasma membrane receptors (e.g. some GPCRs) through second messengers can gate the inositol trisphosphate receptor (InsP3R) in the ER to induce Ca^{2+} release. The levels of Ca^{2+} in the ER then influence store-operated Ca^{2+} entry by plasma membrane Ca^{2+}-release-activated Ca^{2+} (CRAC) channels (with the ORAI pore subunit [187]). Mitochondria are also involved in Ca^{2+} signalling. Many eukaryotes harbour a mitochondrial Ca^{2+} uniporter [188].

The core Ca^{2+} transport systems of ER and plasma membrane channels and pumps have homologues across diverse eukaryotes and were likely present in the LECA. These include SERCA, PMCA, InsP3R, trimeric intracellular cation-specific channels (TRIC) and ORAI [184,189,190]. However, some of the machinery of calcium signalling evolved in the common ancestor of Apusozoa, animals and fungi, representing a post-LECA diversification of ionic signalling (e.g. the sperm-specific CatSper Ca^{2+} channel complex) [191].

Calcium signalling mediates diverse excitable phenomena across eukaryotic taxa. For example, in the ciliate *Tetrahymena*, phagocytosis depends on calcium signalling [192]. In fungi, pulsatile calcium signalling events accompany cellular events, including cell–cell contact and polarized growth [193]. In the slime mould *Dictyostelium*, speed modulation in migrating cells in response to shear stress is dependent on G-protein signalling acting through plasma membrane calcium channels and IP3-mediated internal calcium-store release [29,112,194]. In ciliates, voltage-gated Ca^{2+} channels regulate motility [162] and temperature responses [195].

Besides Ca^{2+}, several other ions are involved in excitability phenomena and are regulated by dedicated pathways. For example, in the *Paramecium* membrane, one study reported six different ionic conductances [196], but there are probably many more, based on the high number of ion channels in the genome [197]. Diatoms and coccolithophores display voltage-activated cation and anion currents [166,198]

Sensory receptor pathways responsible for mediating responses to external cues also originated early in eukaryotes and some were likely present in LECA. These include members of the TRP and GPCR families. TRP channels at the plasma membrane and in the ciliary membrane mediate several excitable phenomena. For example, TRP channels are involved in mechanosensation-induced bioluminescence in the dinoflagellate *Lingulodinium polyedra* [199]. Rheotaxis in shear flow is dependent on a PKD2-like TRP channel in the amoeba *Dictyostelium discoideum* [200]. In the excavate *Euglena gracilis*, Ca^{2+} influx via a mechanosensitive TRP channel mediates negative gravitaxis [201]. In the green alga *Chlamydomonas reinhardtii*, there are several TRP channels involved in various sensory processes. The mechanosensory avoidance reaction of the cells requires the expression of TRP11 localized to the base of flagella [169]. Another flagellar TRP channel, CrPKD2, is important for flagella-dependent mating [202], whereas TRP1 is a thermo-sensitive channel that opens at increased temperatures [203].

Prokaryotes also have channels and transporters involved in various aspects of signalling and cell physiology such as chemotaxis [204–208]. These channels can be homologous to the eukaryotic channels, for example the TRIC channels are conserved across bacteria, archaea and eukaryotes [209]. However, the prokaryotic channels are often simpler and sporadically distributed. For example, most eukaryotic voltage-gated channels are tetrameric whereas prokaryotic channels are monomers [210,211] (but see [166]). The mitochondrial Ca^{2+} uniporter is widespread in eukaryotes but found only sporadically in bacteria [188]. Eukaryotes thus distinguish themselves by the diversity and complexity of channels, pumps and receptors.

(b) Motility by cilia and pseudopodia

There may be as many as 18 distinct motility types across all forms of life [212]. Among these, notable eukaryotic motilities include free-swimming by cilia and migration by pseudopodia. The earliest eukaryote may have been an amoeboflagellate alternating between cilia-driven and amoeboid locomotion. The amoeboid-to-flagellate transition is common among eukaryotes, occurring in Rhizaria [213], Amoebozoa, *Naegleria* [214], several opisthokonts including choanoflagellates [215], filastereans [216] and early-branching fungi [217,218].

These new forms of motility rely on eukaryotic-signature cell biology, including dynamic actin and microtubule cytoskeleton and membrane-bound cilia. Pseudopodia are involved in directional motility, feeding and sensing, as we discussed (in §2b) for the case of chemotaxis in *Dictyostelium* [37]. These actin-filled structures and their regulation by WASP and SCAR proteins trace back to LECA [218]. Here we focus on the uniquely eukaryotic biology of cilia (confusingly, also referred to as flagella in their longer forms) and discuss how they contribute to behaviour and sensing.

We briefly contrast the elaborate regulation, stroke patterns and gait control available for cilia-based motility, with the control of prokaryotic flagella and archaella [219–222]. All three appendage types share some physical similarities. They are all slender structures that create drag anisotropy when moving through a fluid. Net propulsion is achieved by breaking time-reversal symmetry with propagating waves or chiral rotation. Asymmetric interactions also mediate gliding and crawling [223–225].

Beyond these similarities, cilia stand out with a unique propulsion-generating machinery that is very different from that of bacterial flagella or archaella. Bacterial flagella and archaeal archaella are extracellular structures, composed only of a few proteins plus a rotary motor and membrane-embedded base structure, whereas membrane-bound cilia have over 500 proteins [226]. Unlike either of the prokaryotic structures, which are driven by rotary motors from one end, dynein motors populate the entire length of cilia. This is known as distributed force actuation [227], in stark contrast with boundary actuation (from only one end) in the prokaryotic appendages.

The continuity of ciliary membranes as an extension of the plasma membrane enables fast reactions. Active amplification at these locations reduces transduction times from sensor to motor actuators (locomotor appendages), thereby leaving more time for sensory integration or sampling (see §2f). At excitable interfaces, spontaneous fluctuations (due to noisy ion channels) of the resting membrane potential can amplify into action potentials. In flagellates and ciliates, this appears as spontaneous swimming reversals, which can occur in the absence of stimuli [228,229]. Artificial deciliation abolished the calcium-dependent excitability in *Paramecium* [230,231], further highlighting the possible ciliary origin of eukaryotic action potentials [232]. Leveraging mutants defective in ion-gating, several phospholipids were shown to be localized exclusively to the ciliary membrane of *Paramecium* [233].

While prokaryotes can manipulate the sense (and sometimes speed) of flagella rotation, the flexible and distributed architecture of cilia enables many more degrees of freedom. Dynein activity can be modulated intracellularly to produce a spectrum of beating modes within the same structure [234]. For instance, in green algal cilia, calcium induces a switch from a forward swimming mode with an asymmetric waveform (low-frequency) to a reverse mode with a symmetric waveform (high-frequency) in tens of milliseconds [228,235]. The beat pattern and asymmetry of sperm flagella are controlled by calcium and cAMP [236,237].

The capacity for subtle control of ciliary shape and movement underpins the exclusively eukaryotic trait of helical klinotaxis. Multiflagellate algae modulate the parameters of helical trajectories to realign with gradients in a graded, intensity-dependent manner—during *Chlamydomonas* phototaxis, photons incident on the eyespot induce a transient membrane depolarization [168] which alters the flagellar beat pattern [238]. Steering arises when the two flagella respond differently to this signal [239,240].

By contrast, during *E. coli* run-and-tumble, multiple flagella rotate in the same sense during swimming, but unbundling (when one or more motors rotate in the opposite sense) is stochastic. During stochastic chemotaxis, cells can only control the propensity for directional switching but not the new swimming direction. Some prokaryotes (e.g. *Sinorhizobium meliloti*, *Rhodobacter sphaeroides*) can also control motor speed [241–243].

Eukaryotes with multiple cilia can also have fine control over the movement sequence, or gait. This higher-level control requires the precise positioning of centrioles and cilia [244]. Multiciliary coordination can invoke hydrodynamic as well as intracellular means—including electrical signalling [136] or basal-body coupling [245]. Ciliary control dictates the walking gaits of *Euplotes* [246], as well as diverse swimming gaits in algal flagellates, including the breaststroke, trot and gallop. Distinguished cilia on the same cell may be found alternately in sequences of excitation or quiescence [247].

Owing to their larger size and active coordination, cilia can generate faster propulsion and flows. Collectively they can be organized across scales [239,248] for specific tasks. In ciliates and other filter feeders, cilia differentiate into oral cilia for feeding and somatic cilia for swimming. Bioelectrical signalling controls mouth ciliature for complex feeding behaviours, as well as the ciliary beat direction to direct feeding flows [163].

Cilia arose to support not only eukaryotic motility but also sensing [249,250]. The continuity of the membrane around the cilium (and other eukaryotic appendages) is integral to these dual functions. In addition to the various sensory receptors localized to the cilium (discussed in §3a above), cilia and other eukaryotic appendages are sustained out of equilibrium by ATP-dependent mechanochemical cycles, which produce unique dynamical signatures [251,252]. Macroscale flux cycles in the phase space of movement patterns (broken detailed balance) have been observed in cilia [251], in hair cell bundles [253], in the motor patterns of intact swimmers [228] and in reconstituted cytoskeletal networks [253,254]. These exhibit active fluctuations that are orders of magnitude higher than thermal noise and may further enhance sensory perception, particularly to mechanical stimuli and shear flows.

Besides cilia and pseudopodia, cytoskeletal polarization and patterning led to further, highly specialized forms of movement [255]. These involve dynamic mobilization of cellular protrusions for prey capture or manipulation (see §2e). Haptophyte algae have a unique organelle known as a haptonema—a slender microtubular structure distinct from cilia, which coils at high speed to detect prey and other mechanical cues [256]. In *Vorticella* and *Zoothamnium*, contractile proteins in the stalk organelle (spasmoneme) can undergo extremely rapid mechanochemical contraction–extension cycles, fuelled by calcium [257,258]. The axopods of Heliozoa, which are involved in feeding, and contain bundles of microtubules, undergo rapid shortening by microtubule catastrophe [259,260]. In many predatory ciliates, ciliary bundles or cirri form specialized feeding structures that undergo dramatic shape changes to internalize prey.

(c) Origins of mitochondria and endomembranes as intracellular capacitors

The eukaryotic cell is distinguished from prokaryotic cells by a complex endomembrane topology [261–263]. The endomembrane system contains several charged compartments (figure 2*a*)—multiple membranous structures, including the ER, the vacuole and mitochondria, often with closely stacked lamellae (e.g. ER, plastids). This sophisticated structural organization evolved during eukaryogenesis and is critical to eukaryotic excitability.

One important structural innovation was the compartmentalization of chemiosmotic ATP production. In eukaryotes, ATP synthesis occurs in the mitochondria, commonly during aerobic respiration [265]. By contrast, prokaryotes use their plasma membrane for ATP synthesis, where ATP synthase complexes use the transmembrane electrochemical gradient of protons or Na^+ ions [266]. During eukaryogenesis, the original archaeal plasma membrane A_0A_1 ATP synthase [266,267] became internalized, evolving into the vacuolar H^+-ATPase (ATP-driven proton pump), which acidifies vacuoles [268]. Free from the burden of chemiosmotic ATP production, the eukaryotic plasma membrane can now assume novel signalling roles.

Another important aspect of eukaryotic endomembrane organization is the presence of several charged compartments with distinct ionic composition. These distinct compartments function as closed cellular capacitors [269,270]. The compartments are separated by membrane layers with low conductivity that form a physical barrier between the conductive internal and external fluid. These cellular capacitors actively release and replenish charges, gated by channels and pumps, which alter potential differences across membranes. In neurons, the speed of charge propagation from a synapse is inversely proportional to the specific capacitance (C_m, capacitance per unit area of the membrane) of the membrane. For the plasma membrane of animal cells, this is estimated to be approximately 1 $\mu F\ cm^{-2}$ [271].

The ER reversibly stores and releases charge in the form of Ca^{2+} ions. The tunable capacitance of the ER depends on the flow of external ions into the cell by capacitative Ca^{2+} entry [272]. The acidified vacuole is positively charged relative to the cytosol, maintaining a vacuolar capacitance. Mitochondria and chloroplasts with their double membranes have unique capacitative properties (figure 2*b*) [264,273].

We propose that in eukaryotes, the presence of multiple circuits consisting of these capacitors and their gating machineries represents a novel form of information storage and parallel processing not seen in prokaryotes. These capacitors, and the control of their rapid charging and discharging by active currents, form new types of cellular logic gates. The organization of the eukaryotic endomembrane system has three important functional consequences for cellular capacitance. First, the network of thin membranes creates a large surface area for charge storage and high capacitance—bilayer membranes are typically only 5 nm thick. For parallel plates (membranes) of area A separated by thickness d and dielectric constant, ε_0, the capacitance is $C = \varepsilon_0 A/d$. For a spherical capacitor of radius r, this is modified to $C = 4\pi\varepsilon_0 r^2/d$. The capacitance of compressible membranes is also sensitive to mechanical compression; for a 5 nm thick membrane, a 1 nm decrease in thickness can significantly increase capacitance [274].

Second, membrane topology, comprising nested or closely apposed membranes, greatly influences charge distribution. Where multiple membranes are stacked in parallel, resistances add reciprocally, while capacitances add linearly. The placement of different capacitors in a cell influences charge redistribution, particularly during dynamic phenomena such as motility and feeding. Membrane-bound organelles can be as close as 10 nm from the plasma membrane [275].

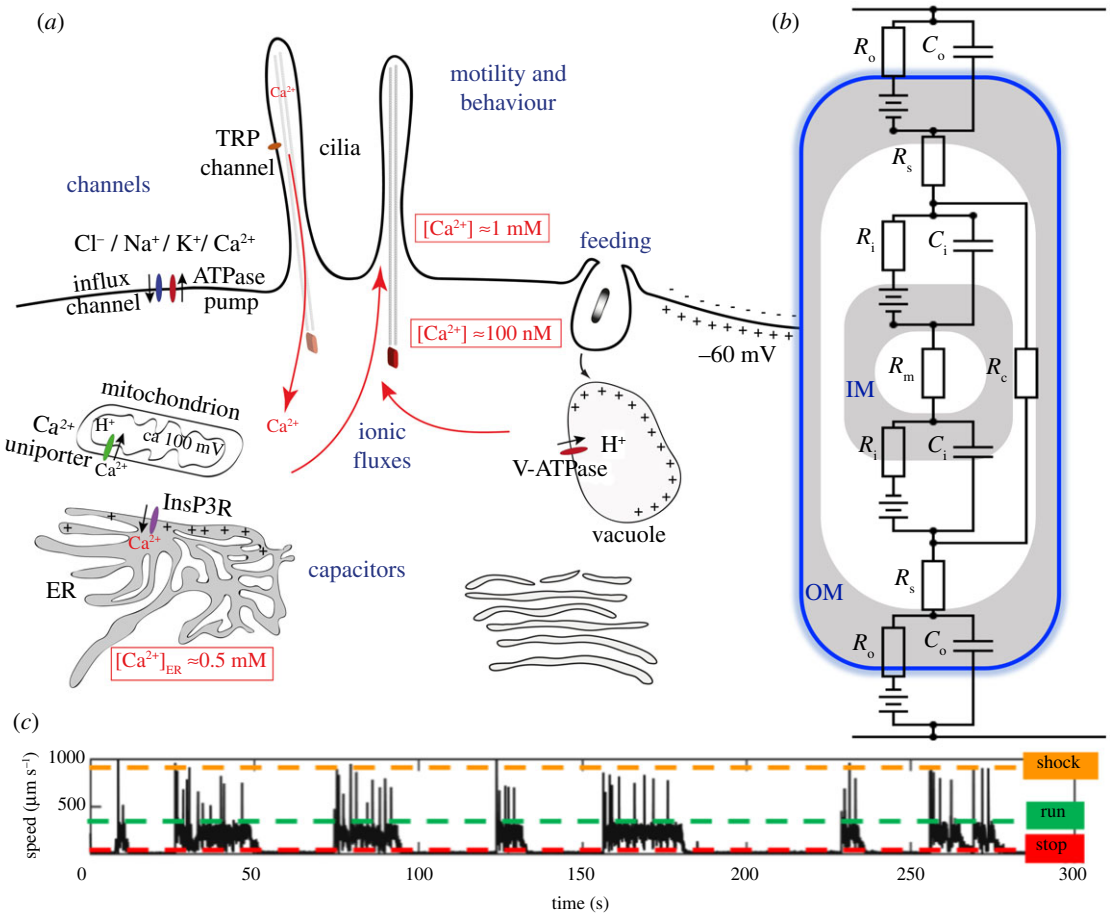

Figure 2. Eukaryotic membranes control dynamic intracellular signalling. (*a*) Massive diversification of lipids and ion channels creates compartments and circuits within a flexible and excitable endomembrane system. (*b*) The mitochondrion has a distinctive two-layer topology with unique capacitative properties (IM, inner membrane; OM, outer membrane; C_i, C_o are IM, OM capacitances; R_i, R_o and R_m are IM, OM and matrix resistances; R_s is the resistance of the inner membrane space; R_c is a 'shunt' resistance [264] arising from cristae extending across the intermembrane space). (*c*) Excitable signalling in cilia manifests as fast transitions or escape responses, as observed here in an octoflagellate protist [228] which switches between three distinct behavioural states (run, stop and shock).

This physical proximity further ensures that coordinated signalling, or cross-talk, can occur near-synchronously across the different compartments. Changes in capacitance were measured in phagocytosing macrophages [275,276].

The third feature of the system is its ability to create and sustain nonlinear cycles of charging and discharging—a form of rapid bioelectric signalling. We illustrate this with a basic bilayer membrane (resistance R, capacitance C); here, the voltage–current relationship is given by [277,278] $V = IR(1 - e^{-t/\tau})$, where $\tau = RC$ is a time constant for capacitative charging and discharging. This is typically of the order of 100 ns, but can be up to microseconds for larger cells [279]. These currents propagate throughout the cell [280], introducing temporal delays and thereby controlling the timing of signalling events, as has been demonstrated in nerve cells [281,282]. The function of multi-organellar capacitative phenomena in excitability remains to be explored experimentally. If such phenomena are important, we would expect them to have a regulatory function, particularly in cells with tightly apposed ionic compartments—for example, in the flagellar pocket and associated membranes (ER, Golgi, mitochondrion, contractile vacuole) of trypanosomes [283], or the various extrusive organelle complexes such as the pellicular system in ciliates, with alveoli, cilia, mitochondria and trichocysts [277,278,284].

We conclude that during eukaryogenesis, the evolution of compartmentalized capacitors significantly increased the degrees of freedom available for intracellular electrical signalling, making critical contributions to eukaryotic excitability and behaviour. This critical function of the complex eukaryotic endomembrane system as a master regulator of behaviour and physiology extends beyond its bioenergetic or metabolic advantages. By analogy with electronics, eukaryotic cells constitute a complex and dynamic network of coupled resistors and interleaved capacitors as charge sources or sinks, which are associated with multiple time constants. Collectively, these circuits and motifs function as timers, frequency filters, tuners and logic gates, whence complex behaviours can ensue.

(d) Flexible and excitable membranes

Except when covered by a cell wall, as are some fungal and plant cells, eukaryotic cells are morphable and undergo shape changes not seen in prokaryotes. One of the key steps of eukaryogenesis was the loss of the rigid glycoprotein cell wall of the archaea-derived host cell [285]. In archaea, the 'rigid structure and extremely tight adhesion or interdigitation of the glycoprotein cell walls […] represent an invincible obstacle' [266, p. 572].

The flexible plasma membrane in eukaryotes was a prerequisite for the evolution of total cell fusion, engulfment and membrane dynamics. The endomembrane system is suggested to have evolved rapidly and the LECA to have possessed an elaborate membrane-trafficking system including

ER, endosomes and stacked Golgi [286]. This was supported by a complex machinery of membrane-sculpting proteins (e.g. SNAREs, small GTPases, ESCRT complex, septins, coatomer), some of it with an origin in the Asgard archaea [287,288]. For example, according to sequence reconstructions, the LECA may have had as many as 23 Rab GTPases [289]. In the absence of a protective cell wall, eukaryotes may have become more prone to localized injury and membrane rupture. This could have contributed to the evolution of membrane repair and recycling mechanisms and excitable signalling [161].

Besides its flexibility, the plasma membrane harbours the greatest diversity of channels and receptors in eukaryotes and—with the inclusion of the highly deformable ciliary membrane—became the most important surface for excitability. Eukaryotic membranes not only have diverse pumps and channels (see §3a above) but also have thousands of distinct lipid species [290] compared with only hundreds in prokaryotic membranes. The same tendency for amphipathic lipids to self-assemble into layers occurs sub-cellularly in eukaryotes to form multiple boundaries that delimit individual organelles. Lipid diversity also encodes organellar identity (different compartments made up of different lipid species), thus preventing them from coalescing. This diversity may have indirectly contributed to maintaining distinct capacitative identities for electrical signalling in organelles.

Enrichment by eukaryotic sterols (particularly cholesterol) and sphingolipids, which form lipid rafts, is a signature eukaryotic trait [291]. Small changes in lipid structure can have dramatic consequences on membrane thermodynamics [292]. Raft clustering and sorting is thought to precede pinching and budding of vesicles, and are critical for membrane and vesicular trafficking. The composition of plasma membranes resides at a critical point [293], which has been proposed to reduce the energetic costs of membrane compartmentalization and reconfiguration. Sterols are also major regulators of the activity of voltage-gated ion channels, which in turn function to alter the capacitance and conductance of eukaryotic membranes [261,294] (see §3c above). A diverse compositional repertoire further ensures that leakage currents can be matched exactly.

Membrane shape depends on a complex interplay of proteins and lipids, and is highly sensitive to the heterogeneous distribution of lipids [295], which promotes the formation of bends and curvatures [296]. Excitability also depends on membrane fluidity [297]. Eukaryotic sterols have a profound effect on fluidity, channel permeability and thickness [298]. Increased membrane fluidity was directly associated with changes in swimming speed in *Tetrahymena* [299]. In nerve membranes, anaesthetics are suggested to alter excitability by altering membrane fluidity [300].

Distortion of a fluid bilayer also provides a unique force-sensing mechanism as a form of membrane mechanosensitivity [301,302]. Shear forces and tension can activate transmembrane mechanosensory channels in a number of organisms, triggering action potentials [303]. Fluid shear has been shown to activate G-proteins [304], as well as increase membrane fluidity in endothelial cells [305] and the light-producing dinoflagellate *Lingulodinium polyedrum* (Alveolata) [306]. In another dinoflagellate, *Pyrocystis lunula*, the critical threshold for bioluminescence was estimated to be approximately 0.1 µN, about thrice the shear stress on the cell wall [307]. Meanwhile the force required to activate rapid behavioural switches (shock response) in a small prasinophyte alga can be under 10 pN [228]. Mechanical stimuli must do work to open transduction channels [308]. The amount of work required is a measure of sensitivity, which is much higher in eukaryotes (table 2). In bullfrog hair bundles, Ca^{2+} can shift the single-channel activation force by approximately 3 pN (equivalent to 1–2 k_BT) [313].

Eukaryotic membranes are capable of significant topological reorganization, notably during wound repair, phagocytosis and cell–cell fusion. Plasma membranes reversibly deform during cell migration or feeding to sustain non-energy-minimizing structures such as slender protrusions [314]. The constant spatio-temporal remodelling and turnover of membranes is a eukaryotic trait. Vigorous membrane turnover is observed in some species of *Acanthamoeba*, at an estimated complete turnover rate of several times per hour [315]. Membrane reorganization, even fusion, can occur between predatory suctorians and their prey [316].

(e) Increase in cell size

If one were allowed to speak of a stereotypical eukaryotic cell, it would be about an order of magnitude larger than a stereotypical prokaryote. Cell size in single-celled eukaryotes ranges from 1 µm [317] to several centimetres (some macroalgae, such as *Acetabularia*), while prokaryotes are typically 1–10 µm and can be diffraction-limited; the smallest mycoplasmas are approximately 0.2 µm [318]. Single-celled eukaryotes are found in most extant phyla. The largest ciliate has approximately 10^6 times the volume of the smallest eukaryote.

Cell size imposes fundamental limits on the ability to generate as well as control self-movement. We highlight two physical consequences of increasing size at the border between prokaryotes and eukaryotes. The first concerns the usefulness of self-movement for migration, while the second, the usefulness of self-generated flows for active feeding or nutrient sensing.

Virtually all single-celled organisms reside at low Reynolds numbers (Re; table 2), where viscosity dominates inertia [319]. At these scales there is no inertial coasting, so organisms stop instantaneously when they stop propelling themselves. Self-movement underlies navigation, active feeding, mating and many forms of excitability (§2, figure 1). However, owing to thermal noise, cells below a critical size can gain no absolute benefit from self-propulsion, regardless of the locomotion mechanism.

To see why, first consider an immotile cell of radius a immersed in a fluid of viscosity μ. It will be subject to Brownian motion, subject to both translational and rotational diffusion. The translational diffusion constant is given by the Stokes–Einstein law $D_0 = k_BT/6\pi\mu a$ and has units of length^2/time, where k_BT ($\approx 4.11 \times 10^{-21}$ J at room temperature) is the thermal energy at temperature T. Meanwhile rotational diffusion $D_r = k_BT/8\pi\mu a^3$ (units of rad^2/time), gives rise to a timescale $\tau = 1/2D_r$ over which the orientation of the cell will be 'reset'.

An actively motile cell will have a higher effective translational diffusion D_a, which depends on the detailed movement strategy, or repertoire [13,17,20]. For run-and-tumble (random reorientations after each tumble), $D_a \approx v^2\tau/3$. For prokaryotes, a typical run speed is $v = 10\ \mu m\ s^{-1}$, and the maximum free-flight time τ can be limited by D_r above. The ratio $D_a/D_0 \sim v^2a^4$ quantifies the benefit of active swimming to

Table 2. Summary of key biophysical scaling relationships. See main text for references and for *rare prokaryotic examples that defy the general trend. (We have assumed throughout: $k_BT = 4.11 \times 10^{-21}$ J = 4.11 pN nm, and $\mu/\rho = 10^{-2}$ cm^2 s^{-1} is the kinematic viscosity of water at room temperature). Symbols are defined in the text.

physical parameter	scaling	(typical) prokaryote	(typical) eukaryote	comments
Reynolds number	$\mathrm{Re} = \rho UL/\mu$	$\mathrm{Re} = 10^{-5}$–10^{-3} (L = 1–10 μm, U = 10–100 μm s^{-1})	$\mathrm{Re} = 10^{-3}$–1 (L = 10–1000 μm, U = 10–1000 μm s^{-1})	unicellular eukaryotes and prokaryotes are viscosity dominated
Péclet number (fix D = 10^3 μm^2 s^{-1} for small molecule)	$\mathrm{Pe} = UL/D$	$\mathrm{Pe} = 10^{-2}$–1 (L, U as above)	$\mathrm{Pe} = 1$–10^3 (L, U as above)	prokaryotes are diffusion-limited and cannot reach* Pe > 1
diffusion constant (passive)	$D_0 = k_BT/(6\pi\mu a)$	$D_0 = 0.22$ μm^2 s^{-1} (a = 1 μm)	$D_0 = 0.02$ μm^2 s^{-1} (a = 10 μm)	eukaryotes 10× less susceptible to linear diffusion
rotational diffusion (passive)	$D_{\mathrm{rot}} = k_BT/(8\pi\mu a^3)$	$D_{\mathrm{rot}} = 0.16$ rad^2 s^{-1} (a = 1 μm)	$D_{\mathrm{rot}} = 1.6 \times 10^{-4}$ rad^2 s^{-1} (a = 10 μm)	eukaryotes 1000× less susceptible to rotational diffusion
effective diffusion (active, depends on motility strategy)	$D_a = v^2\tau/3$ (τ = free-flight time, v = speed of runs)	$D_a \approx 133$ μm^2 s^{-1} ($v \approx 20$ μm s^{-1}, $\tau \approx 1$ s)	$D_a \approx 3.3 \times 10^{-2}$ cm^2 s^{-1} ($v \approx 100$ μm s^{-1}, $\tau \approx 10$ s)	empirical: *E. coli:* [309] $D \approx 10$–100 μm^2 s^{-1}; *C. reinhardtii:* [310] $D \approx 10^{-3}$ cm^2 s^{-1}; *P. caudatum:* [311] $D \approx 10^{-2}$ cm^2 s^{-1}
relevant for stochastic navigation	expected angular deviation in time τ $\theta_{\mathrm{rms}} = \sqrt{(2D_r\tau)}$	$\theta_{\mathrm{rms}} = 32°$ (for $\tau = 1$ s)	$\theta_{\mathrm{rms}} = 1°$ (for $\tau = 1$ s)	prokaryotes are severely limited by rotational diffusion (cannot steer)
relevant for spatial sensing	$\frac{\mathrm{SNR_s}}{\mathrm{SNR_t}} \sim \frac{a}{v\tau}$	too small*	useful strategy for large and slow-moving cells	common strategy for amoeboid eukaryotes
relevant for helical klinotaxis	$\mathrm{SNR_{klinotaxis}} \sim \frac{R^2}{\omega}$	too small*	useful strategy to reorient toward vectorial cues	common strategy for free-swimming eukaryotes
sensitivity to mechanical stimuli (membrane tension)	ratio of channel opening and closing probabilities $\frac{P_0}{P_c} = \exp\left(-\frac{\Delta E}{k_BT}\right)$ ΔE = work done to open channel (approx. sensitivity)	bacterial MscS and MscL channels (osmotic nanovalves): [301] 5 approximately 10 mN m^{-1}	hair cells, single-channel gating stiffness: [308] approximately 1 mN m^{-1} Piezo1: [312] approximately 1.4 mN m^{-1}	1 k_BT is 4 nm^2 change in area under tension of 1 mN m^{-1} lytic tension of pure lipid bilayer approximately 20 mN m^{-1}

passive diffusion, which improves rapidly with increasing size and speed. Dusenbery used this expression to estimate that below a critical radius $a_c \approx 0.64$ µm, active swimming is no longer useful [320]. This may explain the paucity of motile bacteria with radius less than a_c. This motility divide is also present within the green algal order Mamiellophyceae [321], which contains some of the smallest free-living eukaryotes (pico-eukaryotes): the non-motile *Ostreococcus* (approx. 1 µm), and the motile species *Micromonas* (approx. 2 µm), which swims with an average speed of approximately 20 µm s^{-1} [22].

There is thus a dramatic advantage to having even *slightly* larger size. Rotational diffusion D_r determines how much a swimmer can move in a certain direction before a noise-driven trajectory reorientation [322]. For a prokaryote with $a = 1$ µm, $D_r \approx 0.16$ rad^2 s^{-1}, whereas for a eukaryote with $a = 10$ µm, $D_r \approx 10^{-4}$ rad^2 s^{-1}, rotational diffusion is negligible. Active swimming enables eukaryotes to achieve several-fold increase in sensory integration time and self-control over directional persistence (table 2). Eukaryotes can therefore afford to move at higher speeds in order to achieve the same level of signal discrimination (more in §3f).

The second physical consequence concerns how cell size influences solute transport. For a perfect spherical adsorber of radius a, the number of particles (present at ambient

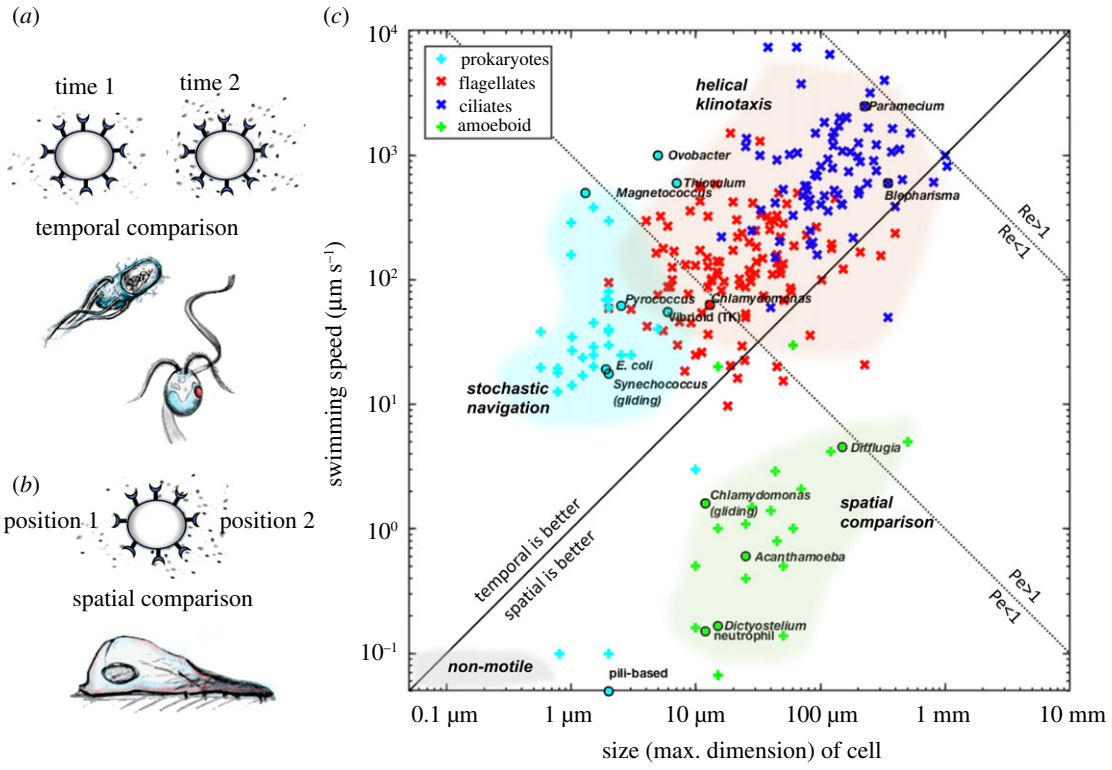

Figure 3. Eukaryotes unlocked new biophysical regimes. (*a*) Temporal sensing strategies typically involve comparing the signal at two slightly different times—this can be stochastic and rotational diffusion limited (as in many prokaryotes), or involve self-steering (as in many ciliates and flagellates). (*b*) Spatial sensing strategies involve comparing the signal at two different positions at the same time (as in most amoeboid cells). (*c*) These distinctions create a prokaryote–eukaryote divide with respect to behaviour, as visualized here in a phase space of organism size versus speed (log–log scale). Three phase boundaries partition this space (see also table 2), namely, the Reynolds number (Re), Péclet number (Pe) and the relative advantage of temporal versus spatial sensing (plotted here for an integration time $\tau = 1$ s). Data points are collated from the literature, where some species of particular interest are highlighted. (In particular see: amoeba [326], flagellates and ciliates [327] and marine bacteria [328]. The full dataset is available as supplementary material.)

concentration C_0) arriving at the surface per unit time is given by $J = 4\pi DC_0a$. Meanwhile an organism's metabolic needs scale much faster, according to volume, or a^3. The energy cost per unit volume of cell required to double the nutrient flux at the cell surface is estimated to be $\sim\mu D^2/a^4$ [323].

This means that while diffusion alone is sufficient to ensure prokaryotes are well-stirred, eukaryotes must have acquired alternative means of advecting flows. Cilia and flagella are often used to create large-scale flows (up to mm s^{-1}) for filter feeding, or for replenishing the local nutrient concentration around cells [324,325]. For a cell with length L, moving at speed U, the importance of advection over diffusion is captured by the Péclet number $\mathrm{Pe} = UL/D$, the ratio between advective (L/U) and diffusive timescales (L^2/D). For a 1 µm prokaryote with a typical speed of 10 µm s^{-1} and $D \approx 10^{-5}$ cm^2 s^{-1} (small molecules), Pe = 0.01, so no physiological amount of movement can improve diffusive uptake. Meanwhile eukaryotes readily achieve Pe numbers of order unity or above (figure 3), so that active stirring is beneficial for nutrient redistribution (mass transfer) and enables scanning through larger volumes of fluid [329].

While there are multiplicitous routes to increasing size and complexity, overcoming the diffusive bottleneck by active transport may have been a key step in eukaryogenesis, and multicellularity. Eukaryotic-signature motilities (dynamic cytoskeleton) also enabled nutrient redistribution inside large cells. Increasing size presents new opportunities for the creation of specialized organelles, such as mitochondria, feeding apparatuses and sensors.

Importantly, most prokaryotes cannot steer deterministically in bulk fluid, nor is it advantageous to do so due to excessive rotational diffusion. Exceptions include a vibrioid bacterium [55], and magnetotatic bacteria including the bilophotrichous *Magnetococcus marinus* [330], and the multicellular magnetotactic prokaryotes (MMPs; approx. 10 µm) [331]. The latter comprise multiple undifferentiated cells whose flagella exhibit some degree of coordination to achieve fast swimming and directional switching, aided by the Earth's magnetic field.

(f) New strategies for sensing and computation

All motile organisms larger than the critical size limit a_c can access new strategies for sampling and sensing their environment beyond simple diffusion. Prokaryotes and eukaryotes use fundamentally distinct motility machinery and have evolved distinct sensing mechanisms (with rare exceptions). Cells are remarkable sensors, able to monitor weak signals with a precision approaching physical limits [332]. Examples include chemoreception in bacteria [333,334] and in sperm [65], photon counting in vision [335] and frequency discrimination in the human ear [336]. It is often physical rather than biological processes that set the limits of cellular sensing and response at the microscale.

Below, we discuss scaling laws that unequivocally constrain sensory fidelity at the microscale. These determine how the sensory signal-to-noise ratio (SNR) depends upon the navigation strategy and the nature of the stimulus,

through parameters such as cell size, swimming speed and sensory integration time. Here, we focus on limits imposed by different strategies for chemosensing and photosensing, and discuss the implications of these limits for cell evolution and the origins of eukaryotic excitability.

Thermal noise is ever-present, arising from molecular encounters (between receptors and ligands), photons, noise in chemical reactions, gene expression etc. Signal detection reduces to stochastic counting of molecules of chemoattractant, or photons (figure 3*a*). For simplicity, we assume that gradients decay exponentially with a length scale ℓ_d. Typically, for chemicals, we can have $\ell_d \approx 0.1$ cm [320]. For light, the length scale will depend more strongly on the medium. We will use the same length scale of $\ell_d \approx 0.1$ cm for simplicity.

For chemosensing, molecules diffuse independently. So the number n of molecules bound by cellular receptors will be Poissonian, $n = 4\pi DC_0\tau a$, where D is the diffusion constant, C_0 the concentration, τ is the available integration or measurement time and a is the cell radius. During spatial sensing of a chemical, cells compare concentrations at two locations separated by $\Delta x = 2a$. Here the signal is $S = (J_+ - J_-)\tau = 6\pi DC_0 a^2\tau/\ell_d$, where $J_\pm$ are the diffusive currents to two halves of a stationary sphere [320]. For a single measurement, the noise is $N = \sqrt{n}$ (Poissonian), with signal-to-noise ratio $SNR_s = S/N \sim a^{3/2}\tau^{1/2}D^{1/2}C_0^{1/2}/\ell_d$. If instead a motile cell moving at speed v performs temporal sensing, $S = C_0\Delta x/\ell_d$, this time $\Delta x = v\tau$ (in the regime $\Delta x \ll \ell_d$). Here, the measurement error is reduced by taking multiple measurements over a time τ, so that $N = C_0(2\pi DC_0 a\tau)^{-1/2}$ [323], and $SNR_t = S/N \sim va^{1/2}\tau^{3/2}D^{1/2}C_0^{1/2}/\ell_d$. Similarly, during photosensing, the photon count $n = IAf\tau$ depends on I, the light intensity (photons per unit area per unit time), the area of the sensor A, the fractional absorbance f ($\ll 1$) and the integration time τ. For spatial comparisons, $N = \sqrt{n}$, so that $SNR_s \sim (IAf\tau)^{1/2}(2a/\ell_d)$. Meanwhile for temporal comparisons, $SNR_t \sim (IAf\tau)^{1/2}v\tau/\ell_d$.

In all cases, the SNR depends strongly on τ. For light or chemical signals, the relative SNR between the two strategies scales similarly (with different prefactors): $SNRs/SNRt \sim a/v\tau$. Similar expressions can be derived for other cues, such as temperature, or for variations upon this sensory strategy [337]. Thus large, slowly moving cells will sense more effectively by spatial comparison, as in large amoeboid eukaryotes which crawl on substrates [29].

By contrast, small fast-moving cells use temporal sensing [338]. Below a certain size (approx. 1 µm), cells become severely limited by rotational diffusion, so prokaryotes cannot maintain their orientation for long enough to steer deterministically toward gradients. Such cells must adopt stochastic random walks. We estimate that in 1 s the expected mean-squared angular displacement, given by $\sqrt{2D_r\tau}$, is about 30° (table 2). Only cells that are large enough can access the third strategy—helical klinotaxis. Here cells rotating around an axis can maintain stable helical swimming. Periodic stroke patterns produce superhelical trajectories over long times [339]. Cells detect gradients perpendicular to the helix axis and gradually steer toward gradients by adjusting the alignment between the swimming direction and gradient (error correction). Receptor organelles and sensors are localized to specific regions of the cell to further increase signal discrimination during active movement. For angular rotation speed ω, we require $\omega \gg D_r$ which sets a minimum cell size for helical klinotaxis: e.g. a cell that rotates once per second about its axis must have a diameter of least 6 µm to achieve $\omega \approx 10D_r$. Thus klinotaxis is not physically accessible for most prokaryotes. Here, the SNR for chemotaxis depends strongly on the signal gradient and scales as $R^2\tau$ where R and τ are the helix radius and period, respectively [340,341].

Eukaryotic cells are in general several times larger than the wavelength of visible light and can use the cell body to focus light. For example, an eye-less strain of *Chlamydomonas* [342] or multicellular *Dictyostelium* slugs [343,344] can focus and align with directional light. In prokaryotes, this mechanism has only been described in cyanobacteria, which operate at the physical limit of focusing [56,345].

In reality, even spatial sensing strategies have a temporal component [346]. Cells measure over a range of timescales, bound by a minimum reaction time and a maximum memory recall. This leads to band-pass signal processing, as has been shown in some bacteria [347]. Since eukaryotes can access a wider range of timescales, they can respond to a wider range of signals. To achieve the same SNR, a larger size can compensate for faster movement, or a shorter reaction time. The entropic and energetic costs of performing cellular computations may have eventually promoted multicellularity or colonial-living, rather than building bigger and more complex single cells. In both pro- and eukaryotes, cell–cell communication can indeed enhance population-level sensing [348,349].

In summary, eukaryotes unlocked novel strategies for improving the sensory SNR. This principally results from an increase in size, polarization of sensors and improved ability to control the swimming direction. The resulting behavioural stratification which partitions the eukaryotes from the prokaryotes can be visualized on a two-dimensional plot of cell size and speed (figure 3*c*).

4. Concluding remarks

With increasing size and structural complexity, eukaryotes developed novel strategies for environmental exploration. Different eukaryotic lineages are characterized by unique combinations of feeding modalities, control pathways and organization of motility appendages. Eukaryote-signature capabilities are most clearly manifest in emergent mechanisms of motility control, particularly of membrane-bound appendages such as cilia. Eukaryotes, thus endowed, became capable of programmed responses to complex stimuli in a more finely tuned manner. In this article, we have identified specific yet universal changes in cellular and membrane architecture that we propose were crucial for such organisms to overcome many of the challenges associated with life and survival.

Though our list may not be exhaustive, it offers a refreshing perspective for tracing the possible scenarios of eukaryogenesis, which emphasizes the need to consider signalling and behaviour at the whole-cell level. As prokaryotes evolved colonial-living (e.g. biofilms) to overcome the bottlenecks encountered at the microscale in terms of sensing and fluid-interactions, single-celled eukaryotes instead were able to attain a level of behavioural sophistication unmatched in single-celled prokaryotes. Given the strong scaling of size with rotational diffusion, we find that even a modest increase in size may have been sufficient to enable greater self-control

and movement persistence (figure 3), and therefore a significant improvement in signal discrimination and decision-making. Such capabilities likely coevolved with cellular and structural innovations.

We suggest that interfacial excitability—the capacity for small potential differences to feed back and suddenly amplify—is critical for the novel functionality of eukaryotic membranes. Although the question of why prokaryotic membranes do not appear to be capable of propagating reproducible, millisecond action potentials remains open, the answer is likely to lie with the massive diversification of proteins and lipids in eukaryotic membranes. We propose that the compositional complexification of eukaryotic membranes conferred excitability to eukaryotes. This diversification enhanced the precision with which control can be exerted over the thermodynamic state of the membrane, its capacitance, fluidity, as well as the identity and magnitude of transmembrane ion fluxes. In this regime, even small changes in physical parameters can feed back and amplify nonlinearly.

In eukaryotes, the integration of fast sensory and excitable motility elements may thus have unlocked new physical regimes of memory and information processing in cells (for example, spatio-temporal navigation requires significant computational bit depth). The capacity to precisely control and generate action potentials, leading to fast escape responses or behavioural transitions, may be a strategy for self-protection from accidental damage. Single-cell neuronal computation [350] may thus have had ancient roots tracing back to ancestral eukaryotes that enacted distributed control over motile appendages [247]. These mechanisms of cellular computation may have been the basis for the origin of nervous systems and more advanced forms of cognition in Metazoa [351]. These concepts are addressed in other contributions in this and the subsequent theme issue on basal cognition.

The acute 'environmental sensibility' of excitable membrane interfaces was probably a key trait of ancestral eukaryotes. Excitability enabled eukaryotes to move, sense, react, feed and finally to fulfil the Biblical injunction, to *multiply* (paraphrasing Mills *et al*. [352]), in radically new ways. It would be hard to escape the conclusion that excitability had a major contribution to the success of eukaryotes and enabled them to conquer all but the most extreme habitats on the planet. What we hope we could also show is that the divide separating eukaryotes from prokaryotes is as wide for excitability and behaviour as for most other cellular features. Future models of eukaryogenesis ought to account for the origins of excitability to paint a fuller picture of this momentous transition in evolution.

Data accessibility. Data collated from published sources were used to generate figure 3*c*. These data are uploaded as electronic supplementary material.

Authors' contributions. K.Y.W. and G.J. wrote the paper.

Competing interests. We declare we have no competing interests.

Funding. K.Y.W. gratefully acknowledges funding from the European Research Council (ERC) under the European Union's Horizon 2020 research and innovation programme under grant agreement no. 853560: 'EvoMotion'—*Moving around without a brain: Evolution of basal cognition in single-celled organisms*. G.J. would like to thank the Leverhulme Trust for funding (RPG-2018-392).

References

1. Izhikevich EM. 2010 *Dynamical systems in neuroscience: the geometry of excitability and bursting*. Cambridge, MA: MIT Press.
2. Gadsby DC. 2009 Ion channels versus ion pumps: the principal difference, in principle. *Nat. Rev. Mol. Cell Biol.* **10**, 344–352. (doi:10.1038/nrm2668)
3. Hodgkin AL, Huxley AF. 1952 A quantitative description of membrane current and its application to conduction and excitation in nerve. *J. Physiol.* **117**, 500–544. (doi:10.1113/jphysiol.1952.sp004764)
4. Poincaré H. 1902 *La science et l'hypothese [Science and hypothesis]*, ch. IX. [In French.] Paris, France: Flammarion.
5. Dusenbery DB. 1992 *Sensory ecology: how organisms acquire and respond to information*. New York, NY: W. H. Freeman & Company.
6. Alvarez L, Friedrich BM, Gompper G, Benjamin Kaupp U. 2014 The computational sperm cell. *Trends Cell Biol.* **24**, 198–207. (doi:10.1016/j.tcb.2013.10.004)
7. Chen Y-R, Zhang R, Du H-J, Pan H-M, Zhang W-Y, Zhou K, Li J-H, Xiao T, Wu L-F. 2015 A novel species of ellipsoidal multicellular magnetotactic prokaryotes from Lake Yuehu in China. *Environ. Microbiol.* **17**, 637–647. (doi:10.1111/1462-2920.12480)
8. Frankel RB, Blakemore RP. 1989 Magnetite and magnetotaxis in microorganisms. *Bioelectromagnetics* **10**, 223–237. (doi:10.1002/bem.2250100303)
9. de Araujo FF, Pires MA, Frankel RB, Bicudo CE. 1986 Magnetite and magnetotaxis in algae. *Biophys. J.* **50**, 375–378. (doi:10.1016/S0006-3495(86)83471-3)
10. Arrieta J, Barreira A, Tuval I. 2015 Microscale patches of nonmotile phytoplankton. *Phys. Rev. Lett.* **114**, 128102. (doi:10.1103/PhysRevLett.114.128102)
11. Gemmell BJ, Oh G, Buskey EJ, Villareal TA. 2016 Dynamic sinking behaviour in marine phytoplankton: rapid changes in buoyancy may aid in nutrient uptake. *Proc. R. Soc. B* **283**, 20161126. (doi:10.1098/rspb.2016.1126)
12. Götz R, Schmitt R. 1987 *Rhizobium meliloti* swims by unidirectional, intermittent rotation of right-handed flagellar helices. *J. Bacteriol.* **169**, 3146–3150. (doi:10.1128/JB.169.7.3146-3150.1987)
13. Berg HC. 1984 *Random walks in biology*, pp. 149–153. Princeton, NJ: Princeton University Press. (doi:10.1515/9781400820023)
14. Adler J. 1965 Chemotaxis in *Escherichia coli*. *Cold Spring Harb. Symp. Quant. Biol.* **30**, 289–292. (doi:10.1101/SQB.1965.030.01.030)
15. Xie L, Altindal T, Chattopadhyay S, Wu X-L. 2011 Bacterial flagellum as a propeller and as a rudder for efficient chemotaxis. *Proc. Natl Acad. Sci. USA* **108**, 2246–2251. (doi:10.1073/pnas.1011953108)
16. Rosser G, Baker RE, Armitage JP, Fletcher AG. 2014 Modelling and analysis of bacterial tracks suggest an active reorientation mechanism in *Rhodobacter sphaeroides*. *J. R. Soc. Interface* **11**, 20140320. (doi:10.1098/rsif.2014.0320)
17. Son K, Guasto JS, Stocker R. 2013 Bacteria can exploit a flagellar buckling instability to change direction. *Nat. Phys.* **9**, 494–498. (doi:10.1038/nphys2676)
18. Rudolph J, Oesterhelt D. 1995 Chemotaxis and phototaxis require a CheA histidine kinase in the archaeon *Halobacterium salinarium*. *EMBO J.* **14**, 667–673. (doi:10.1002/j.1460-2075.1995.tb07045.x)
19. Szurmant H, Ordal GW. 2004 Diversity in chemotaxis mechanisms among the bacteria and archaea. *Microbiol. Mol. Biol. Rev.* **68**, 301–319. (doi:10.1128/MMBR.68.2.301-319.2004)
20. Taktikos J, Stark H, Zaburdaev V. 2013 How the motility pattern of bacteria affects their dispersal and chemotaxis. *PLoS ONE* **8**, e81936. (doi:10.1371/journal.pone.0081936)
21. Kirkegaard JB, Bouillant A, Marron AO, Leptos KC, Goldstein RE. 2016 Aerotaxis in the closest relatives of animals. *eLife* **5**, e18109. (doi:10.7554/eLife.18109)
22. Henshaw R, Jeanneret R, Polin M. 2019. Phototaxis of the dominant marine pico-eukaryote *Micromonas*

sp.: from population to single cell. *bioRxiv*, 740571. (doi:10.1101/740571)

23. Leick V. 1992 Chemotactic properties, cellular binding and uptake of peptides and peptide derivatives: studies with *Tetrahymena thermophila*. *J. Cell Sci.* **103**, 565–570.
24. Van Houten J. 1978 Two mechanisms of chemotaxis in *Paramecium*. *J. Comp. Physiol.* **127**, 167–174. (doi:10.1007/bf01352301)
25. Leick V, Koppelhus U, Rosenberg J. 1994 Cilia-mediated oriented chemokinesis in *Tetrahymena thermophila*. *J. Eukaryot. Microbiol.* **41**, 546–553. (doi:10.1111/j.1550-7408.1994.tb01515.x)
26. Sehring IM, Plattner H. 2004 Ca^{2+} oscillations mediated by exogenous GTP in *Paramecium* cells: assessment of possible Ca^{2+} sources. *Cell Calcium* **36**, 409–420. (doi:10.1016/j.ceca.2004.04.001)
27. Fraenkel GS, Gunn DL. 1940 *The orientation of animals, kineses, taxes and compass reactions*. Oxford, UK: Clarendon Press.
28. Shi C, Iglesias PA. 2013 Excitable behavior in amoeboid chemotaxis. *Wiley Interdiscip. Rev. Syst. Biol. Med.* **5**, 631–642. (doi:10.1002/wsbm.1230)
29. Swaney KF, Huang C-H, Devreotes PN. 2010 Eukaryotic chemotaxis: a network of signaling pathways controls motility, directional sensing, and polarity. *Annu. Rev. Biophys.* **39**, 265–289. (doi:10.1146/annurev.biophys.093008.131228)
30. Marciano-Cabral F, Cline M. 1987 Chemotaxis by *Naegleria fowleri* for bacteria. *J. Protozool.* **34**, 127–131. (doi:10.1111/j.1550-7408.1987.tb03147.x)
31. Schuster FL, Rahman M, Griffith S. 1993 Chemotactic responses of *Acanthamoeba castellanii* to bacteria, bacterial components, and chemotactic peptides. *Trans. Am. Microsc. Soc.* **112**, 43–61. (doi:10.2307/3226781)
32. Urban T, Jarstrand C, Aust-Kettis A. 1983 Migration of *Entamoeba histolytica* under agarose. *Am. J. Trop. Med. Hyg.* **32**, 733–737. (doi:10.4269/ajtmh.1983.32.733)
33. McIntyre J, Jenkin CR. 1969 Chemotaxis in the free living amoeba (*Hartmannella rhysodes*). *Aust. J. Exp. Biol. Med. Sci.* **47**, 625–632. (doi:10.1038/icb.1969.156)
34. Knowles DJ, Carlile MJ. 1978 The chemotactic response of plasmodia of the myxomycete *Physarum polycephalum* to sugars and related compounds. *J. Gen. Microbiol.* **108**, 17–25. (doi:10.1099/00221287-108-1-17)
35. King JS, Insall RH. 2009 Chemotaxis: finding the way forward with *Dictyostelium*. *Trends Cell Biol.* **19**, 523–530. (doi:10.1016/j.tcb.2009.07.004)
36. Skoge M, Yue H, Erickstad M, Bae A, Levine H, Groisman A, Loomis WF, Rappel W-J. 2014 Cellular memory in eukaryotic chemotaxis. *Proc. Natl Acad. Sci. USA* **111**, 14 448–14 453. (doi:10.1073/pnas.1412197111)
37. Andrew N, Insall RH. 2007 Chemotaxis in shallow gradients is mediated independently of PtdIns 3-kinase by biased choices between random protrusions. *Nat. Cell Biol.* **9**, 193–200. (doi:10.1038/ncb1536)
38. Fache S. 2005 Calcium mobilization stimulates *Dictyostelium discoideum* shear-flow-induced cell motility. *J. Cell Sci.* **118**, 3445–3458. (doi:10.1242/jcs.02461)
39. Décavé E, Garrivier D, Bréchet Y, Fourcade B, Bruckert F. 2002 Shear flow-induced detachment kinetics of *Dictyostelium discoideum* cells from solid substrate. *Biophys. J.* **82**, 2383–2395. (doi:10.1016/s0006-3495(02)75583-5)
40. Chen YT. 1950 Investigations of the biology of *Peranema trichophorum* (Euglenineae). *Q. J. Microsc. Sci.* **91**, 279–308.
41. Bloodgood RA. 1988 Gliding motility and the dynamics of flagellar membrane glycoproteins in *Chlamydomonas reinhardtii*. *J. Protozool.* **35**, 552–558. (doi:10.1111/j.1550-7408.1988.tb04151.x)
42. Pringsheim EG. 1968 Kleine Mitteilungen über Flagellaten und Algen [Short contributions on flagellates and algae]. *Arch. Mikrobiol.* **63**, 1–6. [In German.] (doi:10.1007/bf00407057)
43. Ohnuma M, Misumi O, Kuroiwa T. 2011 Phototaxis in the unicellular red algae *Cyanidioschyzon merolae* and *Cyanidium caldarium*. *Cytologia* **76**, 295–300. (doi:10.1508/cytologia.76.295)
44. Maschmann S, Ruban K, Wientapper J, Walter WJ. 2020. Phototaxis of the unicellular red alga *Cyanidioschyzon merolae* is mediated by novel actin-driven tentacles. *Int. J. Mol. Sci.* **21**, 6209. (doi:10.3390/ijms21176209)
45. Sbrana C, Giovannetti M. 2005 Chemotropism in the arbuscular mycorrhizal fungus *Glomus mosseae*. *Mycorrhiza* **15**, 539–545. (doi:10.1007/s00572-005-0362-5)
46. Shimizu KK, Okada K. 2000 Attractive and repulsive interactions between female and male gametophytes in *Arabidopsis* pollen tube guidance. *Development* **127**, 4511–4518.
47. Takahashi H. 1997 Hydrotropism: the current state of our knowledge. *J. Plant Res.* **110**, 163–169. (doi:10.1007/BF02509304)
48. Netotea S, Bertani I, Steindler L, Kerényi A, Venturi V, Pongor S. 2009 A simple model for the early events of quorum sensing in *Pseudomonas aeruginosa*: modeling bacterial swarming as the movement of an 'activation zone'. *Biol. Direct* **4**, 6. (doi:10.1186/1745-6150-4-6)
49. Wilde A, Mullineaux CW. 2017 Light-controlled motility in prokaryotes and the problem of directional light perception. *FEMS Microbiol. Rev.* **41**, 900–922. (doi:10.1093/femsre/fux045)
50. Ragatz L, Jiang ZY, Bauer CE, Gest H. 1995 Macroscopic phototactic behavior of the purple photosynthetic bacterium *Rhodospirillum centenum*. *Arch. Microbiol.* **163**, 1–6. (doi:10.1007/BF00262196)
51. Dworkin M. 1983 Tactic behavior of *Myxococcus xanthus*. *J. Bacteriol.* **154**, 452–459. (doi:10.1128/JB.154.1.452-459.1983)
52. Stanier RY. 1942 A note on elasticotaxis in myxobacteria. *J. Bacteriol.* **44**, 405–412. (doi:10.1128/jb.44.4.405-412.1942)
53. Fontes M, Kaiser D. 1999 *Myxococcus* cells respond to elastic forces in their substrate. *Proc. Natl Acad. Sci. USA* **96**, 8052–8057. (doi:10.1073/pnas.96.14.8052)
54. Muyzer G, Yildirim E, van Dongen U, Kühl M, Thar R. 2005 Identification of "*Candidatus* Thioturbo danicus," a microaerophilic bacterium that builds conspicuous veils on sulfidic sediments. *Appl. Environ. Microbiol.* **71**, 8929–8933. (doi:10.1128/aem.71.12.8929-8933.2005)
55. Thar R, Kuhl M. 2003 Bacteria are not too small for spatial sensing of chemical gradients: an experimental evidence. *Proc. Natl Acad. Sci. USA* **100**, 5748–5753. (doi:10.1073/pnas.1030795100)
56. Schuergers N *et al*. 2016 Cyanobacteria use micro-optics to sense light direction. *eLife* **5**, e12620. (doi:10.7554/eLife.12620)
57. Barbara GM, Mitchell JG. 2003 Bacterial tracking of motile algae. *FEMS Microbiol. Ecol.* **44**, 79–87. (doi:10.1111/j.1574-6941.2003.tb01092.x)
58. Locsei JT, Pedley TJ. 2009 Bacterial tracking of motile algae assisted by algal cell's vorticity field. *Microb. Ecol.* **58**, 63–74. (doi:10.1007/s00248-008-9468-6)
59. Shapere A, Wilczek F. 1989 Geometry of self-propulsion at low Reynolds number. *J. Fluid Mech.* **198**, 557. (doi:10.1017/s002211208900025x)
60. Rossi M, Cicconofri G, Beran A, Noselli G, DeSimone A. 2017 Kinematics of flagellar swimming in *Euglena gracilis*: helical trajectories and flagellar shapes. *Proc. Natl Acad. Sci. USA* **114**, 13 085–13 090. (doi:10.1073/pnas.1708064114)
61. Fenchel T, Blackburn N. 1999 Motile chemosensory behaviour of phagotrophic protists: mechanisms for and efficiency in congregating at food patches. *Protist* **150**, 325–336. (doi:10.1016/S1434-4610(99)70033-7)
62. Tsubo Y. 1961 Chemotaxis and sexual behavior in *Chlamydomonas*. *J. Protozool.* **8**, 114–121. (doi:10.1111/j.1550-7408.1961.tb01191.x)
63. Kinoshita N, Nagasato C, Motomura T. 2017 Phototaxis and chemotaxis of brown algal swarmers. *J. Plant Res.* **130**, 443–453. (doi:10.1007/s10265-017-0914-8)
64. Nultsch W, Häder M. 1984 Light-induced chemotactic responses of the colorless flagellate, *Polytomella magna*, in the presence of photodynamic dyes. *Arch. Microbiol.* **139**, 21–27. (doi:10.1007/bf00692706)
65. Jikeli JF *et al*. 2015 Sperm navigation along helical paths in 3D chemoattractant landscapes. *Nat. Commun.* **6**, 7985. (doi:10.1038/ncomms8985)
66. Pommerville J. 1978 Analysis of gamete and zygote motility in *Allomyces*. *Exp. Cell Res.* **113**, 161–172. (doi:10.1016/0014-4827(78)90096-4)
67. Bowne Jr SW, Bowne GD. 1967 Taxis in *Euglena*. *Exp. Cell Res.* **47**, 545–553. (doi:10.1016/0014-4827(67)90010-9)
68. Häder M. 1984 Light-induced chemotactic reactions in the dinoflagellates, *Peridiniopsis berolinensis*. *Photochem. Photobiol.* **40**, 533–537. (doi:10.1111/j.1751-1097.1984.tb04629.x)
69. Kholodnyy V, Gadêlha H, Cosson J, Boryshpolets S. 2020 How do freshwater fish sperm find the egg? The physicochemical factors guiding the gamete encounters of externally fertilizing freshwater fish. *Rev. Aquac.* **12**, 1165–1192. (doi:10.1111/raq.12378)

70. Satir P, Mitchell DR, Jékely G. 2008 How did the cilium evolve? *Curr. Top. Dev. Biol.* **85**, 63–82. (doi:10.1016/S0070-2153(08)00803-X)
71. Speijer D, Lukeš J, Eliáš M. 2015 Sex is a ubiquitous, ancient, and inherent attribute of eukaryotic life. *Proc. Natl Acad. Sci. USA* **112**, 8827–8834. (doi:10.1073/pnas.1501725112)
72. Muller DG, Jaenicke L, Donike M, Akintobi T. 1971 Sex attractant in a brown alga: chemical structure. *Science* **171**, 815–817. (doi:10.1126/science.171.3973.815)
73. Müller DG, Kawai H, Stache B, Fölster E, Boland W. 1990 Sexual pheromones and gamete chemotaxis in *Analipus japonicus* (Phaeophyceae). *Experientia* **46**, 534–536. (doi:10.1007/bf01954258)
74. Kinoshita N, Shiba K, Inaba K, Fu G, Nagasato C, Motomura T. 2016 Flagellar waveforms of gametes in the brown alga *Ectocarpus siliculosus*. *Eur. J. Phycol.* **51**, 139–148. (doi:10.1080/09670262.2015.1109144)
75. Sugiura M, Shiotani H, Suzaki T, Harumoto T. 2010 Behavioural changes induced by the conjugation-inducing pheromones, gamone 1 and 2, in the ciliate *Blepharisma japonicum*. *Eur. J. Protistol.* **46**, 143–149. (doi:10.1016/j.ejop.2010.01.002)
76. Seshachar BR, Padmavathi PB. 1959 Conjugation in *Spirostomum*. *Nature* **184**, 1510–1511. (doi:10.1038/1841510b0)
77. Stock C, Krüppel T, Key G, Lueken W. 1999 Sexual behaviour in *Euplotes raikovi* is accompanied by pheromone-induced modifications of ionic currents. *J. Exp. Biol.* **202**, 475–483.
78. Jékely G. 2009 Evolution of phototaxis. *Phil. Trans. R. Soc. B* **364**, 2795–2808. (doi:10.1098/rstb.2009.0072)
79. Schaller K, David R, Uhl R. 1997 How *Chlamydomonas* keeps track of the light once it has reached the right phototactic orientation. *Biophys. J.* **73**, 1562–1572. (doi:10.1016/S0006-3495(97)78188-8)
80. Drescher K, Goldstein RE, Tuval I. 2010 Fidelity of adaptive phototaxis. *Proc. Natl Acad. Sci. USA* **107**, 11 171–11 176. (doi:10.1073/pnas.1000901107)
81. Häder D-P. 1993 Simulation of phototaxis in the flagellate *Euglena gracilis*. *J. Biol. Phys.* **19**, 95–108. (doi:10.1007/BF00700253)
82. Tsang ACH, Lam AT, Riedel-Kruse IH. 2018 Polygonal motion and adaptable phototaxis via flagellar beat switching in the microswimmer *Euglena gracilis*. *Nat. Phys.* **14**, 1216–1222. (doi:10.1038/s41567-018-0277-7)
83. Nilsson D-E, Marshall J. 2020 Lens eyes in protists. *Curr. Biol.* **30**, R458–R459. (doi:10.1016/j.cub.2020.01.077)
84. Gavelis GS, Hayakawa S, White III RA, Gojobori T, Suttle CA, Keeling PJ, Leander BS. 2015 Eye-like ocelloids are built from different endosymbiotically acquired components. *Nature* **523**, 204–207. (doi:10.1038/nature14593)
85. Foster KW, Smyth RD. 1980 Light antennas in phototactic algae. *Microbiol. Rev.* **44**, 572–630. (doi:10.1128/MR.44.4.572-630.1980)
86. Gómez F. 2017 The function of the ocelloid and piston in the dinoflagellate *Erythropsidinium* (Gymnodiniales, Dinophyceae). *J. Phycol.* **53**, 629–641. (doi:10.1111/jpy.12525)
87. Darnton NC, Turner L, Rojevsky S, Berg HC. 2007 On torque and tumbling in swimming *Escherichia coli*. *J. Bacteriol.* **189**, 1756–1764. (doi:10.1128/JB.01501-06)
88. Nan B. 2017 Bacterial gliding motility: rolling out a consensus model. *Curr. Biol.* **27**, R154–R156. (doi:10.1016/j.cub.2016.12.035)
89. de Boer W, La Riviere JW, Houwink AL. 1961 Observations on the morphology of *Thiovulum majus* Hinze. *Antonie Van Leeuwenhoek* **27**, 447–456. (doi:10.1007/BF02538470)
90. Garcia-Pichel F. 1989 Rapid bacterial swimming measured in swarming cells of *Thiovulum majus*. *J. Bacteriol.* **171**, 3560–3563. (doi:10.1128/JB.171.6.3560-3563.1989)
91. Thar R, Fenchel T. 2001 True chemotaxis in oxygen gradients of the sulfur-oxidizing bacterium *Thiovulum majus*. *Appl. Environ. Microbiol.* **67**, 3299–3303. (doi:10.1128/AEM.67.7.3299-3303.2001)
92. Petroff A, Libchaber A. 2014 Hydrodynamics and collective behavior of the tethered bacterium *Thiovulum majus*. *Proc. Natl Acad. Sci. USA* **111**, E537–E545. (doi:10.1073/pnas.1322092111)
93. Goodenough U, Heitman J. 2014 Origins of eukaryotic sexual reproduction. *Cold Spring Harb. Perspect. Biol.* **6**, a016154. (doi:10.1101/cshperspect.a016154)
94. Kimball RF. 1942 The nature and inheritance of mating types in *Euplotes patella*. *Genetics* **27**, 269–285.
95. Kitamura A, Hiwatashi K. 1984 Inactivation of cell movement following sexual cell recognition in *Paramecium caudatum*. *Biol. Bull.* **166**, 156–166. (doi:10.2307/1541438)
96. Goodenough UW, Weiss RL. 1975 Gametic differentiation in *Chlamydomonas reinhardtii*. III. Cell wall lysis and microfilament-associated mating structure activation in wild-type and mutant strains. *J. Cell Biol.* **67**, 623–637. (doi:10.1083/jcb.67.3.623)
97. Watanabe T. 1982 Correlation between ventral surface structures and local degeneration of cilia during conjugation in *Paramecium*. *J. Embryol. Exp. Morphol.* **70**, 19–28.
98. Holmes JA, Dutcher SK. 1989 Cellular asymmetry in *Chlamydomonas reinhardtii*. *J. Cell Sci.* **94**, 273–285.
99. Hegemann P, Musgrave A. 1991 Phototaxis of *Chlamydomonas eugametos* pairs is controlled by the mt_+ partner. *J. Plant Physiol.* **138**, 285–291. (doi:10.1016/s0176-1617(11)80289-0)
100. Kreis CT, Le Blay M, Linne C, Makowski MM, Bäumchen O. 2018 Adhesion of *Chlamydomonas* microalgae to surfaces is switchable by light. *Nat. Phys.* **14**, 45–49. (doi:10.1038/nphys4258)
101. Treier U, Fuchs S, Weber M, Wakarchuk WW, Beck CF. 1989 Gametic differentiation in *Chlamydomonas reinhardtii*: light dependence and gene expression patterns. *Arch. Microbiol.* **152**, 572–577. (doi:10.1007/bf00425489)
102. Forbes MA, Hallam ND. 1978 Gamete structure and fertilization in the brown alga *Hormosira banksii* (Turner) Decaisne. *Br. Phycol. J.* **13**, 299–310. (doi:10.1080/00071617800650361)
103. Rosenshine I, Tchelet R, Mevarech M. 1989 The mechanism of DNA transfer in the mating system of an archaebacterium. *Science* **245**, 1387–1389. (doi:10.1126/science.2818746)
104. Shalev Y, Turgeman-Grott I, Tamir A, Eichler J, Gophna U. 2017 Cell surface glycosylation is required for efficient mating of *Haloferax volcanii*. *Front. Microbiol.* **8**, 1253. (doi:10.3389/fmicb.2017.01253)
105. Ducret A, Fleuchot B, Bergam P, Mignot T. 2013 Direct live imaging of cell–cell protein transfer by transient outer membrane fusion in *Myxococcus xanthus*. *eLife* **2**, e00868. (doi:10.7554/elife.00868)
106. Kudryashev M, Cyrklaff M, Alex B, Lemgruber L, Baumeister W, Wallich R, Frischknecht F. 2011 Evidence of direct cell–cell fusion in *Borrelia* by cryogenic electron tomography. *Cell Microbiol.* **13**, 731–741. (doi:10.1111/j.1462-5822.2011.01571.x)
107. Charubin K, Modla S, Caplan JL, Papoutsakis ET. 2020 Interspecies microbial fusion and large-scale exchange of cytoplasmic proteins and RNA in a syntrophic *Clostridium* coculture. *mBio* **11**, e02030-20. (doi:10.1128/mbio.02030-20)
108. Cavalier-Smith T. 2009 Predation and eukaryote cell origins: a coevolutionary perspective. *Int. J. Biochem. Cell Biol.* **41**, 307–322. (doi:10.1016/j.biocel.2008.10.002)
109. Martijn J, Ettema TJG. 2013 From archaeon to eukaryote: the evolutionary dark ages of the eukaryotic cell. *Biochem. Soc. Trans.* **41**, 451–457. (doi:10.1042/BST20120292)
110. Martin WF, Tielens AGM, Mentel M, Garg SG, Gould SB. 2017 The physiology of phagocytosis in the context of mitochondrial origin. *Microbiol. Mol. Biol. Rev.* **81**, e00008-17. (doi:10.1128/MMBR.00008-17)
111. Hausmann K, Bradbury PC (eds). 1996 *Ciliates: cells as organisms*. Stuttgart, Germany: Vch Pub.
112. Pan M, Neilson MP, Grunfeld AM, Cruz P, Wen X, Insall RH, Jin T. 2018 A G-protein-coupled chemoattractant receptor recognizes lipopolysaccharide for bacterial phagocytosis. *PLoS Biol.* **16**, e2005754. (doi:10.1371/journal.pbio.2005754)
113. Pan M, Xu X, Chen Y, Jin T. 2016 Identification of a chemoattractant G-protein-coupled receptor for folic acid that controls both chemotaxis and phagocytosis. *Dev. Cell.* **36**, 428–439. (doi:10.1016/j.devcel.2016.01.012)
114. Wootton EC, Zubkov MV, Jones DH, Jones RH, Martel CM, Thornton CA, Roberts EC. 2007 Biochemical prey recognition by planktonic protozoa. *Environ. Microbiol.* **9**, 216–222. (doi:10.1111/j.1462-2920.2006.01130.x)
115. Hausmann K, Patterson DJ. 1982 Pseudopod formation and membrane production during prey capture by a heliozoon (feeding by *Actinophrys*, II). *Cell Motility* **2**, 9–24. (doi:10.1002/cm.970020103)

116. Leander BS. 2020 Predatory protists. *Curr. Biol.* **30**, R510–R516. (doi:10.1016/j.cub.2020.03.052)
117. Coyle SM, Flaum EM, Li H, Krishnamurthy D, Prakash M. 2019 Coupled active systems encode an emergent hunting behavior in the unicellular predator *Lacrymaria olor*. *Curr. Biol.* **29**, 3838–3850.e3. (doi:10.1016/j.cub.2019.09.034)
118. Breglia SA, Yubuki N, Leander BS. 2013 Ultrastructure and molecular phylogenetic position of *Heteronema scaphurum*: a eukaryovorous euglenid with a cytoproct. *J. Eukaryot. Microbiol.* **60**, 107–120. (doi:10.1111/jeu.12014)
119. Triemer RE. 1997 Feeding in *Peranema trichophorum* revisited (Euglenophyta). *J. Phycol.* **33**, 649–654. (doi:10.1111/j.0022-3646.1997.00649.x)
120. Jacobson DM, Anderson DM. 1986 Thecate heterophic dinoflagellates: feeding behavior and mechanisms. *J. Phycol.* **22**, 249–258. (doi:10.1111/j.1529-8817.1986.tb00021.x)
121. Mast SO. 1909 The reactions of *Didinium nasutum* (Stein) with special reference to the feeding habits and the function of trichocysts. *Biol. Bull.* **16**, 91–118. (doi:10.2307/1536126)
122. Small EB, Marszalek DS. 1969 Scanning electron microscopy of fixed, frozen, and dried protozoa. *Science* **163**, 1064–1065. (doi:10.1126/science.163.3871.1064)
123. Hara R, Asai H, Naitoh Y. 1985 Electrical responses of the carnivorous ciliate *Didinium nasutum* in relation to discharge of the extrusive organelles. *J. Exp. Biol.* **119**, 211–224.
124. Hausmann K, Peck RK. 1979 The mode of function of the cytopharyngeal basket of the ciliate *Pseudomicrothorax dubius*. *Differentiation* **14**, 147–158. (doi:10.1111/j.1432-0436.1979.tb01023.x)
125. Plattner H. 2017 Signalling in ciliates: long- and short-range signals and molecular determinants for cellular dynamics. *Biol. Rev. Camb. Phil. Soc.* **92**, 60–107. (doi:10.1111/brv.12218)
126. Fenchel T. 1980 Suspension feeding in ciliated Protozoa: structure and function of feeding organelles. *Arch. Protist.* **123**, 239–260. (doi:10.1016/s0003-9365(80)80009-1)
127. Pérez J, Moraleda-Muñoz A, Marcos-Torres FJ, Muñoz-Dorado J. 2016 Bacterial predation: 75 years and counting! *Environ. Microbiol.* **18**, 766–779. (doi:10.1111/1462-2920.13171)
128. Rendulic S. 2004 A predator unmasked: life cycle of *Bdellovibrio bacteriovorus* from a genomic perspective. *Science* **303**, 689–692. (doi:10.1126/science.1093027)
129. Jashnsaz H *et al*. 2017 Hydrodynamic hunters. *Biophys. J.* **112**, 1282–1289. (doi:10.1016/j.bpj.2017.02.011)
130. Shiratori T, Suzuki S, Kakizawa Y, Ishida K-I. 2019 Phagocytosis-like cell engulfment by a planctomycete bacterium. *Nat. Commun.* **10**, 5529. (doi:10.1038/s41467-019-13499-2)
131. Mathijssen AJTM, Culver J, Bhamla MS, Prakash M. 2019 Collective intercellular communication through ultra-fast hydrodynamic trigger waves. *Nature* **571**, 560–564. (doi:10.1038/s41586-019-1387-9)
132. Kiørboe T, Jiang H. 2013 To eat and not be eaten: optimal foraging behaviour in suspension feeding copepods. *J. R. Soc. Interface* **10**, 20120693. (doi:10.1098/rsif.2012.0693)
133. Visser AW. 2001 Hydromechanical signals in the plankton. *Mar. Ecol. Prog. Ser.* **222**, 1–24. (doi:10.3354/meps222001)
134. Jakobsen HH. 2002 Escape of protists in predator-generated feeding currents. *Aquat. Microb. Ecol.* **26**, 271–281. (doi:10.3354/ame026271)
135. Jakobsen HH, Everett LM, Strom SL. 2006 Hydromechanical signaling between the ciliate *Mesodinium pulex* and motile protist prey. *Aquat. Microb. Ecol.* **44**, 197–206. (doi:10.3354/ame044197)
136. Naitoh Y, Eckert R. 1969 Ionic mechanisms controlling behavioral responses of *Paramecium* to mechanical stimulation. *Science* **164**, 963–965. (doi:10.1126/science.164.3882.963)
137. Wan KY, Goldstein RE. 2014 Rhythmicity, recurrence, and recovery of flagellar beating. *Phys. Rev. Lett.* **113**, 238103. (doi:10.1103/PhysRevLett.113.238103)
138. Friedrich BM. 2018 Load response of shape-changing microswimmers scales with their swimming efficiency. *Phys. Rev. E* **97**, 042416. (doi:10.1103/PhysRevE.97.042416)
139. Liu P, Lou X, Wingfield JL, Lin J, Nicastro D, Lechtreck K. 2020 *Chlamydomonas* PKD2 organizes mastigonemes, hair-like glycoprotein polymers on cilia. *J. Cell Biol.* **219**, e202001122. (doi:10.1083/jcb.202001122)
140. Häder D-P, Hemmersbach R, Lebert M. 2005 *Gravity and the behavior of unicellular organisms*. Cambridge, UK: Cambridge University Press.
141. Bean B. 1984 Microbial geotaxis. In *Membranes and sensory transduction* (eds G Colombetti, F Lenci), pp. 163–198. Boston, MA: Springer. (doi:10.1007/978-1-4613-2675-5_5)
142. Schuech R, Menden-Deuer S. 2014 Going ballistic in the plankton: anisotropic swimming behavior of marine protists. *Limnol. Oceanogr. Fluids Environ.* **4**, doi:10.1215/21573689-2647998. (doi:10.1215/21573689-2647998)
143. Kage A, Omori T, Kikuchi K, Ishikawa T. 2020 The shape effect of flagella is more important than bottom-heaviness on passive gravitactic orientation in *Chlamydomonas reinhardtii*. *J. Exp. Biol.* **223**, jeb205989. (doi:10.1242/jeb.205989)
144. Guasto JS, Rusconi R, Stocker R. 2012 Fluid mechanics of planktonic microorganisms. *Annu. Rev. Fluid Mech.* **44**, 373–400. (doi:10.1146/annurev-fluid-120710-101156)
145. Bees MA. 2020 Advances in bioconvection. *Annu. Rev. Fluid Mech.* **52**, 449–476. (doi:10.1146/annurev-fluid-010518-040558)
146. Wheeler JD, Secchi E, Rusconi R, Stocker R. 2019 Not just going with the flow: the effects of fluid flow on bacteria and plankton. *Annu. Rev. Cell Dev. Biol.* **35**, 213–237. (doi:10.1146/annurev-cellbio-100818-125119)
147. Kinoshita-Terauchi N, Shiba K, Umezawa T, Matsuda F, Motomura T, Inaba K. 2019 A brown algal sex pheromone reverses the sign of phototaxis by cAMP/Ca_{2+}-dependent signaling in the male gametes of *Mutimo cylindricus* (Cutleriaceae). *J. Photochem. Photobiol. B* **192**, 113–123. (doi:10.1016/j.jphotobiol.2019.01.010)
148. Marcos, Fu HC, Powers TR, Stocker R. 2012 Bacterial rheotaxis. *Proc. Natl Acad. Sci. USA* 109, 4780–4785. (doi:10.1073/pnas.1120955109)
149. Cox CD, Bavi N, Martinac B. 2018 Bacterial mechanosensors. *Annu. Rev. Physiol.* **80**, 71–93. (doi:10.1146/annurev-physiol-021317-121351)
150. Bruni GN, Weekley RA, Dodd BJT, Kralj JM. 2017 Voltage-gated calcium flux mediates *Escherichia coli* mechanosensation. *Proc. Natl Acad. Sci. USA* **114**, 9445–9450. (doi:10.1073/pnas.1703084114)
151. Wadhwa N, Phillips R, Berg HC. 2019 Torque-dependent remodeling of the bacterial flagellar motor. *Proc. Natl Acad. Sci. USA* **116**, 11 764–11 769.
152. Nirody JA, Nord AL, Berry RM. 2019 Load-dependent adaptation near zero load in the bacterial flagellar motor. *J. R. Soc. Interface* **16**, 20190300. (doi:10.1098/rsif.2019.0300)
153. Dufrêne YF, Persat A. 2020 Mechanomicrobiology: how bacteria sense and respond to forces. *Nat. Rev. Microbiol.* **18**, 227–240. (doi:10.1038/s41579-019-0314-2)
154. Jakobsen HH. 2001 Escape response of planktonic protists to fluid mechanical signals. *Mar. Ecol. Prog. Ser.* **214**, 67–78. (doi:10.3354/meps214067)
155. Harumoto T, Miyake A. 1991 Defensive function of trichocysts in *Paramecium*. *J. Exp. Zool.* **260**, 84–92. (doi:10.1002/jez.1402600111)
156. Rosati G, Modeo L. 2003 Extrusomes in ciliates: diversification, distribution, and phylogenetic implications. *J. Eukaryot. Microbiol.* **50**, 383–402. (doi:10.1111/j.1550-7408.2003.tb00260.x)
157. Holland EM, Harz H, Uhl R, Hegemann P. 1997 Control of phobic behavioral responses by rhodopsin-induced photocurrents in *Chlamydomonas*. *Biophys. J.* **73**, 1395–1401. (doi:10.1016/S0006-3495(97)78171-2)
158. Hayashi M, Yagi T, Yoshimura K, Kamiya R. 1998 Real-time observation of Ca^{2+}-induced basal body reorientation in *Chlamydomonas*. *Cell Motil. Cytoskeleton* **41**, 49–56. (doi:10.1002/(sici)1097-0169(1998)41:1)
159. Moriyama Y, Hiyama S, Asai H. 1998 High-speed video cinematographic demonstration of stalk and zooid contraction of *Vorticella convallaria*. *Biophys. J.* **74**, 487–491. (doi:10.1016/s0006-3495(98)77806-3)
160. Ando M, Shigenaka Y. 1989 Structure and function of the cytoskeleton in heliozoa: I. Mechanism of rapid axopodial contraction in *Echinosphaerium*. *Cell Motil. Cytoskeleton* **14**, 288–301. (doi:10.1002/cm.970140214)
161. Brunet T, Arendt D. 2016 From damage response to action potentials: early evolution of neural and contractile modules in stem eukaryotes. *Phil. Trans. R. Soc. B* **371**, 20150043. (doi:10.1098/rstb.2015.0043)
162. Eckert R, Brehm P. 1979 Ionic mechanisms of excitation in *Paramecium*. *Annu. Rev. Biophys. Bioeng.* **8**, 353–383. (doi:10.1146/annurev.bb.08.060179.002033)
163. Eckert R, Naito Y. 1972 Bioelectric control of locomotion in the ciliates. *J. Protozool.* **19**, 237–243. (doi:10.1111/j.1550-7408.1972.tb03444.x)

164. Wood DC. 1982 Membrane permeabilities determining resting, action and mechanoreceptor potentials in *Stentor coeruleus*. *J. Comp. Physiol. A* **146**, 537–550. (doi:10.1007/bf00609450)
165. Taylor AR. 2009 A fast Na^+/Ca^{2+}-based action potential in a marine diatom. *PLoS ONE* **4**, e4966. (doi:10.1371/journal.pone.0004966)
166. Helliwell KE, Chrachri A, Koester JA, Wharam S, Verret F, Taylor AR, Wheeler GL, Brownlee C. 2019 Alternative mechanisms for fast Na^+/Ca^{2+} signaling in eukaryotes via a novel class of single-domain voltage-gated channels. *Curr. Biol.* **29**, 1503–1511.e6. (doi:10.1016/j.cub.2019.03.041)
167. Bingley MS, Thompson CM. 1962 Bioelectric potentials in relation to movement in amoebae. *J. Theor. Biol.* **2**, 16–32. (doi:10.1016/s0022-5193(62)80024-1)
168. Harz H, Hegemann P. 1991 Rhodopsin-regulated calcium currents in *Chlamydomonas*. *Nature* **351**, 489–491. (doi:10.1038/351489a0)
169. Fujiu K, Nakayama Y, Iida H, Sokabe M, Yoshimura K. 2011 Mechanoreception in motile flagella of *Chlamydomonas*. *Nat. Cell Biol.* **13**, 630–632. (doi:10.1038/ncb2214)
170. Fujiu K, Nakayama Y, Yanagisawa A, Sokabe M, Yoshimura K. 2009 *Chlamydomonas* CAV2 encodes a voltage-dependent calcium channel required for the flagellar waveform conversion. *Curr. Biol.* **19**, 133–139. (doi:10.1016/j.cub.2008.11.068)
171. Umbach JA. 1981 *pH and membrane excitability in Paramecium caudatum*. Los Angeles, CA: University of California.
172. Dunlap K. 1977 Localization of calcium channels in *Paramecium caudatum*. *J. Physiol.* **271**, 119–133. (doi:10.1113/jphysiol.1977.sp011993)
173. Echevarria ML, Wolfe GV, Taylor AR. 2016 Feast or flee: bioelectrical regulation of feeding and predator evasion behaviors in the planktonic alveolate *Favella* sp. (Spirotrichia). *J. Exp. Biol.* **219**, 445–456. (doi:10.1242/jeb.121871)
174. Lueken W, Ricci N, Krüppel T. 1996 Rhythmic spontaneous depolarizations determine a slow-and-fast rhythm in walking of the marine hypotrich *Euplotes vannus*. *Eur. J. Protist.* **32**, 47–54. (doi:10.1016/s0932-4739(96)80038-1)
175. Kunita I, Kuroda S, Ohki K, Nakagaki T. 2014 Attempts to retreat from a dead-ended long capillary by backward swimming in *Paramecium*. *Front. Microbiol.* **5**, 270. (doi:10.3389/fmicb.2014.00270)
176. Wood DC. 1988 Habituation in *Stentor*: produced by mechanoreceptor channel modification. *J. Neurosci.* **8**, 2254–2258. (doi:10.1523/JNEUROSCI.08-07-02254.1988)
177. Jennings HS. 1899 Studies on reactions to stimuli in unicellular organisms. III Reactions to localized stimuli in *Spirostomum* and *Stentor*. *Am. Nat.* **33**, 373–389. (doi:10.1086/277256)
178. Dexter JP, Prabakaran S, Gunawardena J. 2019 A complex hierarchy of avoidance behaviors in a single-cell eukaryote. *Curr. Biol.* **29**, 4323–4329.e2. (doi:10.1016/j.cub.2019.10.059)
179. Yang C-Y, Bialecka-Fornal M, Weatherwax C, Larkin JW, Prindle A, Liu J, Garcia-Ojalvo J, Süel GM. 2020 Encoding membrane-potential-based memory within a microbial community. *Cell Syst.* **10**, 417–423.e3. (doi:10.1016/j.cels.2020.04.002)
180. Grishanin RN, Bibikov SI, Altschuler IM, Kaulen AD, Kazimirchuk SB, Armitage JP, Skulachev VP. 1996 delta psi-mediated signalling in the bacteriorhodopsin-dependent photoresponse. *J. Bacteriol.* **178**, 3008–3014. (doi:10.1128/JB.178.11.3008-3014.1996)
181. Williams TA, Cox CJ, Foster PG, Szöllősi GJ, Embley TM. 2020 Phylogenomics provides robust support for a two-domains tree of life. *Nat. Ecol. Evol.* **4**, 138–147. (doi:10.1038/s41559-019-1040-x)
182. Zachar I, Szathmáry E. 2017 Breath-giving cooperation: critical review of origin of mitochondria hypotheses. *Biol. Direct* **12**, 19. (doi:10.1186/s13062-017-0190-5)
183. López-García P, Moreira D. 2020 The syntrophy hypothesis for the origin of eukaryotes revisited. *Nat. Microbiol.* **5**, 655–667. (doi:10.1038/s41564-020-0710-4)
184. Schäffer DE, Iyer LM, Burroughs AM, Aravind L. 2020 Functional innovation in the evolution of the calcium-dependent system of the eukaryotic endoplasmic reticulum. *Front. Genet.* **11**, 34. (doi:10.3389/fgene.2020.00034)
185. Jackson AP *et al*. 2016 Kinetoplastid phylogenomics reveals the evolutionary innovations associated with the origins of parasitism. *Curr. Biol.* **26**, 161–172. (doi:10.1016/j.cub.2015.11.055)
186. Stathopulos PB, Ikura M. 2017 Store operated calcium entry: from concept to structural mechanisms. *Cell Calcium* **63**, 3–7. (doi:10.1016/j.ceca.2016.11.005)
187. Prakriya M, Feske S, Gwack Y, Srikanth S, Rao A, Hogan PG. 2006 Orai1 is an essential pore subunit of the CRAC channel. *Nature* **443**, 230–233. (doi:10.1038/nature05122)
188. Bick AG, Calvo SE, Mootha VK. 2012 Evolutionary diversity of the mitochondrial calcium uniporter. *Science* **336**, 886. (doi:10.1126/science.1214977)
189. Alzayady KJ, Sebé-Pedrós A, Chandrasekhar R, Wang L, Ruiz-Trillo I, Yule DI. 2015 Tracing the evolutionary history of inositol, 1, 4, 5-trisphosphate receptor: insights from analyses of *Capsaspora owczarzaki* Ca^{2+} release channel orthologs. *Mol. Biol. Evol.* **32**, 2236–2253. (doi:10.1093/molbev/msv098)
190. Plattner H, Verkhratsky A. 2015 The ancient roots of calcium signalling evolutionary tree. *Cell Calcium* **57**, 123–132. (doi:10.1016/j.ceca.2014.12.004)
191. Cai X, Clapham DE. 2012 Ancestral Ca^{2+} signaling machinery in early animal and fungal evolution. *Mol. Biol. Evol.* **29**, 91–100. (doi:10.1093/molbev/msr149)
192. Gonda K, Komatsu M, Numata O. 2000 Calmodulin and Ca^{2+}/calmodulin-binding proteins are involved in *Tetrahymena thermophila* phagocytosis. *Cell Struct. Funct.* **25**, 243–251. (doi:10.1247/csf.25.243)
193. Kim H-S, Czymmek KJ, Patel A, Modla S, Nohe A, Duncan R, Gilroy S, Kang S. 2012 Expression of the Cameleon calcium biosensor in fungi reveals distinct Ca^{2+} signatures associated with polarized growth, development, and pathogenesis. *Fungal Genet. Biol.* **49**, 589–601. (doi:10.1016/j.fgb.2012.05.011)
194. Chen M-Y, Insall RH, Devreotes PN. 1996 Signaling through chemoattractant receptors in *Dictyostelium*. *Trends Genet.* **12**, 52–57. (doi:10.1016/0168-9525(96)81400-4)
195. Kuriu T, Saitow F, Nakaoka Y, Oosawa Y. 1998 Calcium current activated by cooling in *Paramecium*. *J. Comp. Physiol. A* **183**, 135–141. (doi:10.1007/s003590050241)
196. Kung C, Saimi Y. 1982 The physiological basis of taxes in *Paramecium*. *Annu. Rev. Physiol.* **44**, 519–534. (doi:10.1146/annurev.ph.44.030182.002511)
197. Martinac B, Saimi Y, Kung C. 2008 Ion channels in microbes. *Physiol. Rev.* **88**, 1449–1490. (doi:10.1152/physrev.00005.2008)
198. Taylor AR, Brownlee C. 2003 A novel Cl^- inward-rectifying current in the plasma membrane of the calcifying marine phytoplankton *Coccolithus pelagicus*. *Plant Physiol.* **131**, 1391–1400. (doi:10.1104/pp.011791)
199. Lindström JB, Pierce NT, Latz MI. 2017 Role of TRP channels in dinoflagellate mechanotransduction. *Biol. Bull.* **233**, 151–167. (doi:10.1086/695421)
200. Lima WC, Vinet A, Pieters J, Cosson P. 2014 Role of PKD2 in rheotaxis in *Dictyostelium*. *PLoS ONE* **9**, e88682. (doi:10.1371/journal.pone.0088682)
201. Häder D-P, Hemmersbach R. 2017 Gravitaxis in *Euglena*. *Adv. Exp. Med. Biol.* **979**, 237–266. (doi:10.1007/978-3-319-54910-1_12)
202. Huang K, Diener DR, Mitchell A, Pazour GJ, Witman GB, Rosenbaum JL. 2007 Function and dynamics of PKD2 in *Chlamydomonas reinhardtii* flagella. *J. Cell Biol.* **179**, 501–514. (doi:10.1083/jcb.200704069)
203. McGoldrick LL, Singh AK, Demirkhanyan L, Lin T-Y, Casner RG, Zakharian E, Sobolevsky AI. 2019 Structure of the thermo-sensitive TRP channel TRP1 from the alga *Chlamydomonas reinhardtii*. *Nat. Commun.* **10**, 4180. (doi:10.1038/s41467-019-12121-9)
204. Domínguez DC, Guragain M, Patrauchan M. 2015 Calcium binding proteins and calcium signaling in prokaryotes. *Cell Calcium* **57**, 151–165. (doi:10.1016/j.ceca.2014.12.006)
205. Domínguez DC. 2018 Calcium signaling in prokaryotes. *Calcium Signal Transduct.* (doi:10.5772/intechopen.78546)
206. Tisa LS, Adler J. 1995 Cytoplasmic free-Ca^{2+} level rises with repellents and falls with attractants in *Escherichia coli* chemotaxis. *Proc. Natl Acad. Sci. USA* **92**, 10 777–10 781. (doi:10.1073/pnas.92.23.10777)
207. Ordal GW. 1977 Calcium ion regulates chemotactic behaviour in bacteria. *Nature* **270**, 66–67. (doi:10.1038/270066a0)
208. Ordaq GW, Fields RB. 1977 A biochemical mechanism for bacterial chemotaxis. *J. Theor. Biol.* **68**, 491–500. (doi:10.1016/0022-5193(77)90100-x)
209. Silverio ALF, Saier Jr MH. 2011 Bioinformatic characterization of the trimeric intracellular cation-specific channel protein family. *J. Membr. Biol.* **241**, 77–101. (doi:10.1007/s00232-011-9364-8)

210. Fux JE, Mehta A, Moffat J, Spafford JD. 2018 Eukaryotic voltage-gated sodium channels: on their origins, asymmetries, losses, diversification and adaptations. *Front. Physiol.* **9**, 1406. (doi:10.3389/fphys.2018.01406)
211. Durell SR, Guy HR. 2001 A putative prokaryote voltage-gated Ca^{2+} channel with only one 6TM motif per subunit. *Biochem. Biophys. Res. Commun.* **281**, 741–746. (doi:10.1006/bbrc.2001.4408)
212. Miyata M *et al*. 2020 Tree of motility – a proposed history of motility systems in the tree of life. *Genes Cells* **25**, 6–21. (doi:10.1111/gtc.12737)
213. Cavalier-Smith T, Chao EE, Lewis R. 2018 Multigene phylogeny and cell evolution of chromist infrakingdom Rhizaria: contrasting cell organisation of sister phyla Cercozoa and Retaria. *Protoplasma* **255**, 1517–1574. (doi:10.1007/s00709-018-1241-1)
214. Fritz-Laylin LK *et al*. 2010 The genome of *Naegleria gruberi* illuminates early eukaryotic versatility. *Cell* **140**, 631–642. (doi:10.1016/j.cell.2010.01.032)
215. Brunet T, Albert M, Roman W, Spitzer DC, King N. 2020 A flagellate-to-amoeboid switch in the closest living relatives of animals. *bioRxiv*, 2020.06.26.171736. (doi:10.1101/2020.06.26.171736)
216. Tikhonenkov DV, Hehenberger E, Esaulov AS, Belyakova OI, Mazei YA, Mylnikov AP, Keeling PJ. 2020 Insights into the origin of metazoan multicellularity from predatory unicellular relatives of animals. *BMC Biol.* **18**, 39. (doi:10.1186/s12915-020-0762-1)
217. Karpov SA, Vishnyakov AE, Moreira D, López-García P. 2019 The ultrastructure of *Sanchytrium tribonematis* (Sanchytriaceae, Fungi *incertae sedis*) confirms its close relationship to *Amoeboradix*. *J. Eukaryot. Microbiol.* **66**, 892–898. (doi:10.1111/jeu.12740)
218. Fritz-Laylin LK, Lord SJ, Dyche Mullins R. 2017 WASP and SCAR are evolutionarily conserved in actin-filled pseudopod-based motility. *J. Cell Biol.* **216**, 1673–1688. (doi:10.1083/jcb.201701074)
219. Alam M, Oesterhelt D. 1984 Morphology, function and isolation of halobacterial flagella. *J. Mol. Biol.* **176**, 459–475. (doi:10.1016/0022-2836(84)90172-4)
220. Lowe G, Meister M, Berg HC. 1987 Rapid rotation of flagellar bundles in swimming bacteria. *Nature* **325**, 637–640. (doi:10.1038/325637a0)
221. Albers S-V, Jarrell KF. 2018 The archaellum: an update on the unique archaeal motility structure. *Trends Microbiol.* **26**, 351–362. (doi:10.1016/j.tim.2018.01.004)
222. Albers S-V, Jarrell KF. 2015 The archaellum: how Archaea swim. *Front. Microbiol.* **6**, 23. (doi:10.3389/fmicb.2015.00023)
223. Mullins RD. 2010 Cytoskeletal mechanisms for breaking cellular symmetry. *Cold Spring Harb. Perspect. Biol.* **2**, a003392. (doi:10.1101/cshperspect.a003392)
224. Poulsen NC, Spector I, Spurck TP, Schultz TF, Wetherbee R. 1999 Diatom gliding is the result of an actin-myosin motility system. *Cell Motil. Cytoskeleton* **44**, 23–33. (doi:10.1002/(SICI)1097-0169(199909)44:1<23::AID-CM2>3.0.CO;2-D)
225. Lewis OL, Zhang S, Guy RD, del Álamo JC. 2015 Coordination of contractility, adhesion and flow in migrating *Physarum* amoebae. *J. R. Soc. Interface* **12**, 20141359. (doi:10.1098/rsif.2014.1359)
226. Beeby M, Ferreira JL, Tripp P, Albers S-V, Mitchell DR. 2020 Propulsive nanomachines: the convergent evolution of archaella, flagella, and cilia. *FEMS Microbiol. Rev.* **44**, 253–304. (doi:10.1093/femsre/fuaa006)
227. Machin KE. 1958 Wave propagation along flagella. *J. Exp. Biol.* **35**, 796–806.
228. Wan KY, Goldstein RE. 2018 Time irreversibility and criticality in the motility of a flagellate microorganism. *Phys. Rev. Lett.* **121**, 058103. (doi:10.1103/PhysRevLett.121.058103)
229. Moolenaar WH, De Goede J, Verveen AA. 1976 Membrane noise in *Paramecium*. *Nature* **260**, 344–346. (doi:10.1038/260344a0)
230. Nakaoka Y, Imaji T, Hara M, Hashimoto N. 2009 Spontaneous fluctuation of the resting membrane potential in *Paramecium*: amplification caused by intracellular Ca^{2+}. *J. Exp. Biol.* **212**, 270–276. (doi:10.1242/jeb.023283)
231. Machemer H, Ogura A. 1979 Ionic conductances of membranes in ciliated and deciliated *Paramecium*. *J. Physiol.* **296**, 49–60. (doi:10.1113/jphysiol.1979.sp012990)
232. Ogura A, Takahashi K. 1976 Artificial deciliation causes loss of calcium-dependent responses in *Paramecium*. *Nature* **264**, 170–172. (doi:10.1038/264170a0)
233. Eisenbach L, Ramanathan R, Nelson DL. 1983 Biochemical studies of the excitable membrane of *Paramecium tetraurelia*. IX. Antibodies against ciliary membrane proteins. *J. Cell Biol.* **97**, 1412–1420. (doi:10.1083/jcb.97.5.1412)
234. Sleigh MA, Barlow DI. 1982 How are different ciliary beat patterns produced? *Symp. Soc. Exp. Biol.* **35**, 139–157.
235. Schmidt JA, Eckert R. 1976 Calcium couples flagellar reversal to photostimulation in *Chlamydomonas reinhardtii*. *Nature* **262**, 713–715. (doi:10.1038/262713a0)
236. Lindemann CB, Kanous KS. 1989 Regulation of mammalian sperm motility. *Arch. Androl.* **23**, 1–22. (doi:10.3109/01485018908986783)
237. Jansen V, Alvarez L, Balbach M, Strünker T, Hegemann P, Kaupp UB, Wachten D. 2015 Controlling fertilization and cAMP signaling in sperm by optogenetics. *eLife* **4**, e05161. (doi:10.7554/eLife.05161)
238. Kamiya R, Witman GB. 1984 Submicromolar levels of calcium control the balance of beating between the two flagella in demembranated models of *Chlamydomonas*. *J. Cell Biol.* **98**, 97–107. (doi:10.1083/jcb.98.1.97)
239. Wan KY. 2018 Coordination of eukaryotic cilia and flagella. *Essays Biochem.* **62**, 829–838. (doi:10.1042/EBC20180029)
240. Isogai N, Kamiya R, Yoshimura K. 2000 Dominance between the two flagella during phototactic turning in *Chlamydomonas*. *Zool. Sci.* **17**, 1261–1266. (doi:10.2108/zsj.17.1261)
241. Schmitt R. 2002 Sinorhizobial chemotaxis: a departure from the enterobacterial paradigm. *Microbiology* **148**, 627–631. (doi:10.1099/00221287-148-3-627)
242. Platzer J, Sterr W, Hausmann M, Schmitt R. 1997 Three genes of a motility operon and their role in flagellar rotary speed variation in *Rhizobium meliloti*. *J. Bacteriol.* **179**, 6391–6399. (doi:10.1128/JB.179.20.6391-6399.1997)
243. Packer HL, Lawther H, Armitage JP. 1997 The *Rhodobacter sphaeroides* flagellar motor is a variable-speed rotor. *FEBS Lett.* **409**, 37–40. (doi:10.1016/S0014-5793(97)00473-0)
244. Bornens M. 2018 Cell polarity: having and making sense of direction—on the evolutionary significance of the primary cilium/centrosome organ in Metazoa. *Open Biol.* **8**, 180052. (doi:10.1098/rsob.180052)
245. Wan KY, Goldstein RE. 2016 Coordinated beating of algal flagella is mediated by basal coupling. *Proc. Natl Acad. Sci. USA* **113**, E2784–E2793. (doi:10.1073/pnas.1518527113)
246. Erra F, Iervasi A, Ricci N, Banchetti R. 2001 Movement of the cirri during the creeping of *Euplotes crassus* (Ciliata, Hypotrichida). *Can. J. Zool.* **79**, 1353–1362. (doi:10.1139/z01-030)
247. Wan KY. 2020 Synchrony and symmetry-breaking in active flagellar coordination. *Phil. Trans. R. Soc. B* **375**, 20190393. (doi:10.1098/rstb.2019.0393)
248. Gilpin W, Bull MS, Prakash M. 2020 The multiscale physics of cilia and flagella. *Nat. Rev. Phys.* **2**, 74–88. (doi:10.1038/s42254-019-0129-0)
249. Jékely G. 2011 Origin and early evolution of neural circuits for the control of ciliary locomotion. *Proc. R. Soc. B* **278**, 914–922. (doi:10.1098/rspb.2010.2027)
250. Carvalho-Santos Z, Azimzadeh J, Pereira-Leal JB, Bettencourt-Dias M. 2011 Evolution: tracing the origins of centrioles, cilia, and flagella. *J. Cell Biol.* **194**, 165–175. (doi:10.1083/jcb.201011152)
251. Battle C, Broedersz CP, Fakhri N, Geyer VF, Howard J, Schmidt CF, MacKintosh FC. 2016 Broken detailed balance at mesoscopic scales in active biological systems. *Science* **352**, 604–607. (doi:10.1126/science.aac8167)
252. Gnesotto FS, Mura F, Gladrow J, Broedersz CP. 2018 Broken detailed balance and non-equilibrium dynamics in living systems: a review. *Rep. Prog. Phys.* **81**, 066601. (doi:10.1088/1361-6633/aab3ed)
253. Martin P, Hudspeth AJ, Julicher F. 2001 Comparison of a hair bundle's spontaneous oscillations with its response to mechanical stimulation reveals the underlying active process. *Proc. Natl Acad. Sci. USA* **98**, 14 380–14 385. (doi:10.1073/pnas.251530598)
254. Brangwynne CP, Koenderink GH, MacKintosh FC, Weitz DA. 2008 Nonequilibrium microtubule fluctuations in a model cytoskeleton. *Phys. Rev. Lett.* **100**, 118104. (doi:10.1103/physrevlett.100.118104)
255. Marshall WF. 2020 Pattern formation and complexity in single cells. *Curr. Biol.* **30**, R544–R552. (doi:10.1016/j.cub.2020.04.011)
256. Nomura M, Atsuji K, Hirose K, Shiba K, Yanase R, Nakayama T, Ishida K-I, Inaba K. 2019 Microtubule stabilizer reveals requirement of Ca-dependent conformational changes of microtubules for rapid

coiling of haptonema in haptophyte algae. *Biol. Open* **8**, bio036590. (doi:10.1242/bio.036590)

257. Katoh K, Kikuyama M. 1997 An all-or-nothing rise in cytosolic. *J. Exp. Biol.* **200**, 35–40.
258. Amos WB. 1971 Reversible mechanochemical cycle in the contraction of *Vorticella*. *Nature* **229**, 127–128. (doi:10.1038/229127a0)
259. Tilney LG, Porter KR. 1965 Studies on microtubules in Heliozoa. I. The fine structure of *Actinosphaerium nucleofilum* (Barrett), with particular reference to the axial rod structure. *Protoplasma* **60**, 317–344. (doi:10.1007/BF01247886)
260. Febvre-Chevalier C, Febvre J. 1992 Microtubule dissassembly in vivo: intercalary destabilization and breakdown of microtubules in the heliozoan *Actinocoryne contractilis*. *J. Cell Biol.* **118**, 585–594. (doi:10.1083/jcb.118.3.585)
261. Balajthy A, Hajdu P, Panyi G, Varga Z. 2017 Sterol regulation of voltage-gated K channels. *Curr. Top. Membr.* **80**, 255–292. (doi:10.1016/bs.ctm.2017.05.006)
262. Gould SB. 2018 Membranes and evolution. *Curr. Biol.* **28**, R381–R385. (doi:10.1016/j.cub.2018.01.086)
263. Terasaki M *et al*. 2013 Stacked endoplasmic reticulum sheets are connected by helicoidal membrane motifs. *Cell* **154**, 285–296. (doi:10.1016/j.cell.2013.06.031)
264. Padmaraj D, Pande R, Miller JH, Wosik J, Zagozdzon-Wosik W. 2014 Mitochondrial membrane studies using impedance spectroscopy with parallel pH monitoring. *PLoS ONE* **9**, e101793. (doi:10.1371/journal.pone.0101793)
265. Roger AJ, Muñoz-Gómez SA, Kamikawa R. 2017 The origin and diversification of mitochondria. *Curr. Biol.* **27**, R1177–R1192. (doi:10.1016/j.cub.2017.09.015)
266. Schäfer G, Engelhard M, Müller V. 1999 Bioenergetics of the Archaea. *Microbiol. Mol. Biol. Rev.* **63**, 570–620. (doi:10.1128/MMBR.63.3.570-620.1999)
267. Lewalter K, Müller V. 2006 Bioenergetics of archaea: ancient energy conserving mechanisms developed in the early history of life. *Biochim. Biophys. Acta* **1757**, 437–445. (doi:10.1016/j.bbabio.2006.04.027)
268. Gogarten JP *et al*. 1989 Evolution of the vacuolar H^+-ATPase: implications for the origin of eukaryotes. *Proc. Natl Acad. Sci. USA* **86**, 6661–6665. (doi:10.1073/pnas.86.17.6661)
269. Ray S, Kassan A, Busija AR, Rangamani P, Patel HH. 2016 The plasma membrane as a capacitor for energy and metabolism. *Am. J. Physiol. Cell Physiol.* **310**, C181–C192. (doi:10.1152/ajpcell.00087.2015)
270. Everitt CT, Haydon DA. 1968 Electrical capacitance of a lipid membrane separating two aqueous phases. *J. Theor. Biol.* **18**, 371–379. (doi:10.1016/0022-5193(68)90084-2)
271. Gentet LJ, Stuart GJ, Clements JD. 2000 Direct measurement of specific membrane capacitance in neurons. *Biophys. J.* **79**, 314–320. (doi:10.1016/S0006-3495(00)76293-X)
272. Locke EG, Bonilla M, Liang L, Takita Y, Cunningham KW. 2000 A homolog of voltage-gated Ca^{2+} channels stimulated by depletion of secretory Ca^{2+} in yeast. *Mol. Cell. Biol.* **20**, 6686–6694. (doi:10.1128/MCB.20.18.6686-6694.2000)
273. Carraretto L, Teardo E, Checchetto V, Finazzi G, Uozumi N, Szabo I. 2016 Ion channels in plant bioenergetic organelles, chloroplasts and mitochondria: from molecular identification to function. *Mol. Plant* **9**, 371–395. (doi:10.1016/j.molp.2015.12.004)
274. Heimburg T. 2012 The capacitance and electromechanical coupling of lipid membranes close to transitions: the effect of electrostriction. *Biophys. J.* **103**, 918–929. (doi:10.1016/j.bpj.2012.07.010)
275. Pichler H, Gaigg B, Hrastnik C, Achleitner G, Kohlwein SD, Zellnig G, Perktold A, Daum G. 2001 A subfraction of the yeast endoplasmic reticulum associates with the plasma membrane and has a high capacity to synthesize lipids. *Eur. J. Biochem.* **268**, 2351–2361. (doi:10.1046/j.1432-1327.2001.02116.x)
276. Holevinsky KO, Nelson DJ. 1998 Membrane capacitance changes associated with particle uptake during phagocytosis in macrophages. *Biophys. J.* **75**, 2577–2586. (doi:10.1016/S0006-3495(98)77703-3)
277. Hausmann K. 1978 Extrusive organelles in protists. *Int. Rev. Cytol.* **52**, 197–276. (doi:10.1016/S0074-7696(08)60757-3)
278. Stelly N, Halpern S, Nicolas G, Fragu P, Adoutte A. 1995 Direct visualization of a vast cortical calcium compartment in *Paramecium* by secondary ion mass spectrometry (SIMS) microscopy: possible involvement in exocytosis. *J. Cell Sci.* **108**, 1895–1909.
279. Frey W, White JA, Price RO, Blackmore PF, Joshi RP, Nuccitelli R, Beebe SJ, Schoenbach KH, Kolb JF. 2006 Plasma membrane voltage changes during nanosecond pulsed electric field exposure. *Biophys. J.* **90**, 3608–3615. (doi:10.1529/biophysj.105.072777)
280. Schoenbachk KH, Joshi RP, Kolb JF, Chen N, Stacey M, Buescher ES, Beebe SJ, Blackmon P. 2005 Ultrashort electrical pulses open a new gateway into biological cells. In *Conf. Rec. 26th Int. Power Modulator Symp. 2004 and 2004 High-Voltage Workshop, San Francisco, CA, 2004*, pp. 205–209. Piscataway, NJ: IEEE. (doi:10.1109/modsym.2004.1433545)
281. Rall W. 1959 Branching dendritic trees and motoneuron membrane resistivity. *Exp. Neurol.* **1**, 491–527. (doi:10.1016/0014-4886(59)90046-9)
282. Jaeger D, De Schutter E, Bower JM. 1997 The role of synaptic and voltage-gated currents in the control of Purkinje cell spiking: a modeling study. *J. Neurosci.* **17**, 91–106. (doi:10.1523/JNEUROSCI.17-01-00091.1997)
283. Lacomble S, Vaughan S, Gadelha C, Morphew MK, Shaw MK, McIntosh JR, Gull K. 2009 Three-dimensional cellular architecture of the flagellar pocket and associated cytoskeleton in trypanosomes revealed by electron microscope tomography. *J. Cell Sci.* **122**, 1081–1090. (doi:10.1242/jcs.045740)
284. Kugrens P, Lee RE, Corliss JO. 1994 Ultrastructure, biogenesis, and functions of extrusive organelles in selected non-ciliate protists. *Protoplasma* **181**, 164–190. (doi:10.1007/bf01666394)
285. Cavalier-Smith T. 2014 The neomuran revolution and phagotrophic origin of eukaryotes and cilia in the light of intracellular coevolution and a revised tree of life. *Cold Spring Harb. Perspect. Biol.* **6**, a016006. (doi:10.1101/cshperspect.a016006)
286. Dacks JB, Field MC. 2007 Evolution of the eukaryotic membrane-trafficking system: origin, tempo and mode. *J. Cell Sci.* **120**, 2977–2985. (doi:10.1242/jcs.013250)
287. Zaremba-Niedzwiedzka K *et al*. 2017 Asgard archaea illuminate the origin of eukaryotic cellular complexity. *Nature* **541**, 353–358. (doi:10.1038/nature21031)
288. Neveu E, Khalifeh D, Salamin N, Fasshauer D. 2020 Prototypic SNARE proteins are encoded in the genomes of Heimdallarchaeota, potentially bridging the gap between the prokaryotes and eukaryotes. *Curr. Biol.* **30**, 2468–2480.e5. (doi:10.1016/j.cub.2020.04.060)
289. Elias M, Brighouse A, Gabernet-Castello C, Field MC, Dacks JB. 2012 Sculpting the endomembrane system in deep time: high resolution phylogenetics of Rab GTPases. *J. Cell Sci.* **125**, 2500–2508. (doi:10.1242/jcs.101378)
290. Simons K, Sampaio JL. 2011 Membrane organization and lipid rafts. *Cold Spring Harb. Perspect. Biol.* **3**, a004697. (doi:10.1101/cshperspect.a004697)
291. Rasmussen B, Fletcher IR, Brocks JJ, Kilburn MR. 2008 Reassessing the first appearance of eukaryotes and cyanobacteria. *Nature* **455**, 1101–1104. (doi:10.1038/nature07381)
292. Klose C, Ejsing CS, García-Sáez AJ, Kaiser H-J, Sampaio JL, Surma MA, Shevchenko A, Schwille P, Simons K. 2010 Yeast lipids can phase-separate into micrometer-scale membrane domains. *J. Biol. Chem.* **285**, 30 224–30 232. (doi:10.1074/jbc.M110.123554)
293. Honerkamp-Smith AR, Veatch SL, Keller SL. 2009 An introduction to critical points for biophysicists; observations of compositional heterogeneity in lipid membranes. *Biochim. Biophys. Acta Biomembranes* **1788**, 53–63. (doi:10.1016/j.bbamem.2008.09.010)
294. Levitan I, Fang Y, Rosenhouse-Dantsker A, Romanenko V. 2010 Cholesterol and ion channels. *Subcell. Biochem.* **51**, 509–549. (doi:10.1007/978-90-481-8622-8_19)
295. Heimburg T, Jackson AD. 2005 On soliton propagation in biomembranes and nerves. *Proc. Natl Acad. Sci. USA* **102**, 9790–9795. (doi:10.1073/pnas.0503823102)
296. Prinz WA, Hinshaw JE. 2009 Membrane-bending proteins. *Crit. Rev. Biochem. Mol. Biol.* **44**, 278–291. (doi:10.1080/10409230903183472)
297. Corda D, Pasternak C, Shinitzky M. 1982 Increase in lipid microviscosity of unilamellar vesicles upon the creation of transmembrane potential. *J. Membr. Biol.* **65**, 235–242. (doi:10.1007/BF01869967)
298. Bolotina V, Omelyanenko V, Heyes B, Ryan U, Bregestovski P. 1989 Variations of membrane cholesterol alter the kinetics of Ca^{2+}-dependent K^+ channels and membrane fluidity in vascular smooth

muscle cells. *Pflugers Arch.* **415**, 262–268. (doi:10.1007/BF00370875)

299. Goto M, Ohki K, Nozawa Y. 1982 Evidence for a correlation between swimming velocity and membrane fluidity of *Tetrahymena* cells. *Biochim. Biophys. Acta* **693**, 335–340. (doi:10.1016/0005-2736(82)90440-0)
300. Lee AG. 1976 Model for action of local anaesthetics. *Nature* **262**, 545–548. (doi:10.1038/262545a0)
301. Kung C, Martinac B, Sukharev S. 2010 Mechanosensitive channels in microbes. *Annu. Rev. Microbiol.* **64**, 313–329. (doi:10.1146/annurev.micro.112408.134106)
302. Keren K. 2011 Cell motility: the integrating role of the plasma membrane. *Eur. Biophys. J.* **40**, 1013–1027. (doi:10.1007/s00249-011-0741-0)
303. Zimmermann U, Beckers F. 1978 Generation of action potentials in *Chara corallina* by turgor pressure changes. *Planta* **138**, 173–179. (doi:10.1007/BF00391175)
304. Gudi S, Nolan JP, Frangos JA. 1998 Modulation of GTPase activity of G proteins by fluid shear stress and phospholipid composition. *Proc. Natl Acad. Sci. USA* **95**, 2515–2519. (doi:10.1073/pnas.95.5.2515)
305. Haidekker MA, L'Heureux N, Frangos JA. 2000 Fluid shear stress increases membrane fluidity in endothelial cells: a study with DCVJ fluorescence. *Am. J. Physiol. Heart Circ. Physiol.* **278**, H1401–H1406. (doi:10.1152/ajpheart.2000.278.4.H1401)
306. Mallipattu SK, Haidekker MA, Von Dassow P, Latz MI, Frangos JA. 2002 Evidence for shear-induced increase in membrane fluidity in the dinoflagellate *Lingulodinium polyedrum*. *J. Comp. Physiol. A Neuroethol. Sens. Neural Behav. Physiol.* **188**, 409–416. (doi:10.1007/s00359-002-0315-9)
307. Jalaal M, Schramma N, Dode A, de Maleprade H, Raufaste C, Goldstein RE. 2020 Stress-induced dinoflagellate bioluminescence at the single cell level. *Phys. Rev. Lett.* **125**, 028102. (doi:10.1103/PhysRevLett.125.028102)
308. Hudspeth AJ, Choe Y, Mehta AD, Martin P. 2000 Putting ion channels to work: mechanoelectrical transduction, adaptation, and amplification by hair cells. *Proc. Natl Acad. Sci. USA* 97, 11 765–11 772. (doi:10.1073/pnas.97.22.11765)
309. Patteson AE, Gopinath A, Goulian M, Arratia PE. 2015 Running and tumbling with *E. coli* in polymeric solutions. *Scient. Rep.* **5**, 15761. (doi:10.1038/srep15761)
310. Polin M, Tuval I, Drescher K, Gollub JP, Goldstein RE. 2009 *Chlamydomonas* swims with two 'gears' in a eukaryotic version of run-and-tumble locomotion. *Science* 325, 487–490. (doi:10.1126/science.1172667)
311. Kawakubo T, Tsuchiya Y. 1981 Diffusion coefficient of *Paramecium* as a function of temperature1. *J. Protozool.* **28**, 342–344. (doi:10.1111/j.1550-7408.1981.tb02862.x)
312. Lewis AH, Grandl J. 2015 Mechanical sensitivity of Piezo1 ion channels can be tuned by cellular membrane tension. *eLife* **4**, e12088. (doi:10.7554/eLife.12088)
313. Cheung ELM, Corey DP. 2006 Ca^{2+} changes the force sensitivity of the hair-cell transduction channel. In *Auditory mechanisms: processes and models* (eds AL Nuttall, T Ren, P Gillespie, K Grosh, E de Boer), pp. 277–285. Singapore: World Scientific. (doi:10.1142/9789812773456_0047)
314. Jékely G, Arendt D. 2006 Evolution of intraflagellar transport from coated vesicles and autogenous origin of the eukaryotic cilium. *Bioessays* **28**, 191–198. (doi:10.1002/bies.20369)
315. Bowers B, Olszewski TE. 1972 Pinocytosis in *Acanthamoeba castellanii*. Kinetics and morphology. *J. Cell Biol.* **53**, 681–694. (doi:10.1083/jcb.53.3.681)
316. Benwitz G. 1984 Die Entladung der Haptocysten von *Ephelota gemmipara* (Suctoria, Ciliata) [Mode of discharge of haptocysts in *Ephelota gemmipara* (Suctoria, Ciliata)]. *Z. Naturforsch. C* **39**, 812–817. [In German with English abstract.] (doi:10.1515/znc-1984-7-821)
317. Derelle E *et al*. 2006 Genome analysis of the smallest free-living eukaryote *Ostreococcus tauri* unveils many unique features. *Proc. Natl Acad. Sci. USA* **103**, 11 647–11 652. (doi:10.1073/pnas.0604795103)
318. Razin S. 1992 Peculiar properties of mycoplasmas: the smallest self-replicating prokaryotes. *FEMS Microbiol. Lett.* **100**, 423–431. (doi:10.1111/j.1574-6968.1992.tb05735.x)
319. Purcell EM. 1976 Life at low Reynolds number. *AIP Conf. Proc.* **28**, 49–64. (doi:10.1063/1.30370)
320. Dusenbery DB. 1997 Minimum size limit for useful locomotion by free-swimming microbes. *Proc. Natl Acad. Sci. USA* **94**, 10 949–10 954. (doi:10.1073/pnas.94.20.10949)
321. Marin B, Melkonian M. 2010 Molecular phylogeny and classification of the Mamiellophyceae class. nov. (Chlorophyta) based on sequence comparisons of the nuclear- and plastid-encoded rRNA operons. *Protist* **161**, 304–336. (doi:10.1016/j.protis.2009.10.002)
322. Taylor GI. 1922 Diffusion by continuous movements. *Proc. Lond. Math. Soc.* **s2-20**, 196–212. (doi:10.1112/plms/s2-20.1.196)
323. Berg HC, Purcell EM. 1977 Physics of chemoreception. *Biophys. J.* **20**, 193–219. (doi:10.1016/s0006-3495(77)85544-6)
324. Higdon JJL. 1979 The generation of feeding currents by flagellar motions. *J. Fluid Mech.* **94**, 305–330. (doi:10.1017/s002211207900104x)
325. Wan KY, Hürlimann SK, Fenix AM, McGillivary RM, Makushok T, Burns E, Sheung JY, Marshall WF. 2020 Reorganization of complex ciliary flows around regenerating Stentor coeruleus. *Phil. Trans. R. Soc. B* **375**, 20190167. (doi:10.1098/rstb.2019.0167)
326. Claussen M, Schmidt S. 2017 Locomotion pattern and pace of free-living amoebae - a microscopic study. In *Microscopy and imaging science: practical approaches to applied research and education* (ed. A Mendez-Vilas), pp. 223–230. Badajoz, Spain: Formatex Research Center.
327. Lisicki M, Velho Rodrigues MF, Goldstein RE, Lauga E. 2019 Swimming eukaryotic microorganisms exhibit a universal speed distribution. *eLife* **8**, e44907. (doi:10.7554/eLife.44907)
328. Johansen JE, Pinhassi J, Blackburn N, Zweifel UL, Hagström Å. 2002 Variability in motility characteristics among marine bacteria. *Aquat. Microbiol. Ecol.* **28**, 229–237. (doi:10.3354/ame028229)
329. Childress S, Koehl MAR, Miksis M. 1987 Scanning currents in Stokes flow and the efficient feeding of small organisms. *J. Fluid Mech.* **177**, 407–436. (doi:10.1017/s0022112087001022)
330. Bente K, Mohammadinejad S, Charsooghi MA, Bachmann F, Codutti A, Lefèvre CT, Klumpp S, Faivre D. 2020 High-speed motility originates from cooperatively pushing and pulling flagella bundles in bilophotrichous bacteria. *eLife* **9**, e47551. (doi:10.7554/eLife.47551)
331. Winklhofer M, Abraçado LG, Davila AF, Keim CN, de Barros HGPL. 2007 Magnetic optimization in a multicellular magnetotactic organism. *Biophys. J.* **92**, 661–670. (doi:10.1529/biophysj.106.093823)
332. Bialek W. 1987 Physical limits to sensation and perception. *Annu. Rev. Biophys. Biophys. Chem.* **16**, 455–478. (doi:10.1146/annurev.bb.16.060187.002323)
333. Bicknell BA, Dayan P, Goodhill GJ. 2015 The limits of chemosensation vary across dimensions. *Nat. Commun.* **6**, 7468. (doi:10.1038/ncomms8468)
334. Endres RG, Wingreen NS. 2008 Accuracy of direct gradient sensing by single cells. *Proc. Natl Acad. Sci. USA* **105**, 15 749–15 754. (doi:10.1073/pnas.0804688105)
335. Rieke F, Baylor DA. 1998 Single-photon detection by rod cells of the retina. *Rev. Mod. Phys.* **70**, 1027–1036. (doi:10.1103/revmodphys.70.1027)
336. Hudspeth AJ. 1983 The hair cells of the inner ear. *Scient. Am.* **248**, 54–64. (doi:10.1038/scientificamerican0183-54)
337. Tan RZ, Chiam K-H. 2018 A computational model for how cells choose temporal or spatial sensing during chemotaxis. *PLoS Comput. Biol.* **14**, e1005966. (doi:10.1371/journal.pcbi.1005966)
338. Dusenbery DB. 1998 Spatial sensing of stimulus gradients can be superior to temporal sensing for free-swimming bacteria. *Biophys. J.* **74**, 2272–2277. (doi:10.1016/S0006-3495(98)77936-6)
339. Cortese D, Wan KY. 2020 Control of helical navigation by three-dimensional flagellar beating. *BioRxiv*, 2020.09.27.315606. (doi:10.1101/2020.09.27.315606)
340. Kromer JA, Märcker S, Lange S, Baier C, Friedrich BM. 2018 Decision making improves sperm chemotaxis in the presence of noise. *PLoS Comput. Biol.* **14**, e1006109. (doi:10.1371/journal.pcbi.1006109)
341. Friedrich BM, Jülicher F. 2009 Steering chiral swimmers along noisy helical paths. *Phys. Rev. Lett.* **103**, 068102. (doi:10.1103/PhysRevLett.103.068102)
342. Ueki N *et al*. 2016 Eyespot-dependent determination of the phototactic sign in *Chlamydomonas reinhardtii*. *Proc. Natl Acad. Sci. USA* **113**, 5299–5304. (doi:10.1073/pnas.1525538113)
343. Miura K, Siegert F. 2000 Light affects cAMP signaling and cell movement activity in *Dictyostelium discoideum*. *Proc. Natl Acad. Sci. USA* **97**, 2111–2116. (doi:10.1073/pnas.040554497)

344. Francis DW. 1964 Some studies on phototaxis of *Dictyostelium*. *J. Cell. Comp. Physiol.* **64**, 131–138. (doi:10.1002/jcp.1030640113)
345. Nilsson D-E, Colley NJ. 2016 Comparative vision: can bacteria really see? *Curr. Biol.* **26**, R369–R371. (doi:10.1016/j.cub.2016.03.025)
346. Tweedy L, Thomason PA, Paschke PI, Martin K, Machesky LM, Zagnoni M, Insall RH. 2020 Seeing around corners: cells solve mazes and respond at a distance using attractant breakdown. *Science* **369**, eaay9792. (doi:10.1126/science.aay9792)
347. Segall JE, Block SM, Berg HC. 1986 Temporal comparisons in bacterial chemotaxis. *Proc. Natl Acad. Sci. USA* **83**, 8987–8991. (doi:10.1073/pnas.83.23.8987)
348. Fancher S, Mugler A. 2017 Fundamental limits to collective concentration sensing in cell populations. *Phys. Rev. Lett.* **118**, 078101. (doi:10.1103/physrevlett.118.078101)
349. Mehta P, Goyal S, Long T, Bassler BL, Wingreen NS. 2009 Information processing and signal integration in bacterial quorum sensing. *Mol. Syst. Biol.* **5**, 325. (doi:10.1038/msb.2009.79)
350. London M, Häusser M. 2005 Dendritic computation. *Annu. Rev. Neurosci.* **28**, 503–532. (doi:10.1146/annurev.neuro.28.061604.135703)
351. Cook ND, Carvalho GB, Damasio A. 2014 From membrane excitability to metazoan psychology. *Trends Neurosci.* **37**, 698–705. (doi:10.1016/j.tins.2014.07.011)
352. Mills DR, Peterson RL, Spiegelman S. 1967 An extracellular Darwinian experiment with a self-duplicating nucleic acid molecule. *Proc. Natl Acad. Sci. USA* **58**, 217–224. (doi:10.1073/pnas.58.1.217)